Energy Conversion and Management: X 26 (2025) 100937

Contents lists available at ScienceDirect

Energy Conversion and Management: X

journal homepage: www.sciencedirect.com/journal/energy-conversion-and-management-x

# Operational implications of transporting hydrogen via a high-pressure gas network

Amirreza Azimipoor [a,*], Tong Zhang [a,b], Meysam Qadrdan [a], Nick Jenkins [a]

[a] School of Engineering, Cardiff University, Cardiff, UK
[b] School of Engineering, University of Leeds, Leeds, UK

ARTICLE INFO

*Keywords:*
Hydrogen-Natural Gas Transmission
Gas Network
Component Tracing
Transient Simulation

ABSTRACT

Transporting hydrogen gas has long been identified as one of the key issues to scaling up the hydrogen economy. Among various means of transportation, many countries are considering using the existing natural gas pipeline networks for hydrogen transmission. This paper examines the implications of transporting hydrogen on the operational metrics of the high-pressure natural gas networks. A model of the GB high-pressure gas network was developed, which has a high granularity, with 294 nodes, 356 pipes, and 24 compressor stations. The model was developed using Synergi Gas, a hydraulic pipeline network simulation software. By performing unsteady-state analysis, pressure levels, linepack levels and compressor energy consumption were simulated with 10-minute time steps. Additionally, component tracing analysis was utilised to examine the variations in gas composition when hydrogen is injected into the gas network. Five scenarios were developed: one benchmark scenario representing the network transporting natural gas in 2018; one scenario where demand and supply levels are projected for 2035, but no hydrogen was transported by the network; two hydrogen injection scenarios in 2035 considering different geographical locations for hydrogen injection into the gas network; and lastly, one pure hydrogen transmission scenario for 2050. The studies found that the GB's high-pressure gas network could accept 20 % volumetric hydrogen injection without significantly impacting network operation. Pressure levels and compressor energy consumption remain within the operational range. The geographical distribution of hydrogen injection points would highly affect the percentage of hydrogen across the network. Pure hydrogen transportation will cause significant variations in network linepack and increase compressor energy consumption significantly compared to other case studies. The findings signal that operating a network with pure hydrogen is possible only when it is prepared for these changes.

## 1. Introduction

Under the Paris Climate Accords, 195 countries committed to reducing greenhouse gas emissions to maintain global surface temperature increases below 2° Celcuis [1]. Most European countries enacted legally binding legislation targeting net-zero emissions by 2050 to meet this goal [2,3].

Countries in Europe with established natural gas industries see hydrogen ($H_2$) gas as a crucial means of achieving their net-zero targets [4,5]. Many of the industries that consume natural gas, have the potential to convert to use $H_2$ gas instead. Heavy industries which utilise high-temperature processes, like the steel industry, can convert to using blends of $H_2$ and natural gas [6,7]. Also, heavy-goods vehicles and large cargo ships will replace conventional fuels with various forms of $H_2$ fuel [8,9]. It is anticipated that $H_2$ gas can also be used for power generation by 2050 [8,10]. Furthermore, households in parts of Europe may use $H_2$ gas for heating when other low-carbon heating methods prove ineffective [6,8,11].

$H_2$ gas is also valued as a means of energy storage. Excess energy produced by intermittent renewable sources, such as wind, can be converted into $H_2$ gas via electrolysis and stored long-term in salt caverns and depleted gas wells[12]. Hydrogen can also be stored short-term in the natural gas pipeline network [13].

Transporting hydrogen is a key component of these strategies. A key European Commission study examined various methods for hydrogen transportation, concluding that pipelines are the most viable option for transporting 100,000 tonnes of hydrogen over distances less than 3,000 km [14]. More recent research also confirms the view that the most economically viable option for hydrogen transportation is via pipelines

* Corresponding author.
*E-mail address:* AzimipoorA@cardiff.ac.uk (A. Azimipoor).

https://doi.org/10.1016/j.ecmx.2025.100937
Received 21 October 2024; Received in revised form 30 January 2025; Accepted 18 February 2025
Available online 19 February 2025

## Nomenclature

*Abbreviations*

| | |
|---|---|
| Bar-g | Bars-gauged(pressure unit equal to $10^5$ Pa) |
| BWRS | Benedict-Webb-Rubin-Starling |
| CCGT | Combined-cycle gas turbine |
| CCS | Carbon Capture and Storage |
| EHB | European Hydrogen Backbone |
| ESO | Electricity System Operator |
| FES | Future Energy Scenarios (a document published by the GB national energy system operator, NESO. |
| GTYS | Gas Ten-Year Statement (published annually by National Gas, the GB gas transmission operator) |
| GWh | Gigawatt-hourGiga Watt Hour |
| IQR | Interquartile Range |
| LDZ | Local Distribution Zone (receiving gas from the high-pressure gas network)_ |
| LNG | Liquified Natural Gas |
| $Mm^3/d$ | Millions of Standard Cubic Meters per Day |
| $Mm^3/h$ | Millions of Standard Cubic Meters per Hour |
| MWh | Megawatt- hour |
| NTS | National Transmission System (the GB high-pressure gas network) |
| P2G | Power to Gas (for hydrogen production) |
| SMR | Steam Methane Reformation (for hydrogen production) |
| Vol | Volumetric |

*Symbols*

| | |
|---|---|
| A | The cross-sectional area of the pipe [$m^2$] |
| a | Gas flow exponent [1.3] |
| D | Diameter [m] |
| d | Day (as a unit of time) |
| $\varepsilon$ | Absolute roughness of a pipe [ assumed 0.067 mm] |
| $F$ | Frictional force |
| $h$ | Hour (as a unit of time) |
| $H_2$ | Hydrogen molecule |
| $k_F$ | Friction factor of pipe |
| $k_{ij}$ | Interaction coefficient of components $i$ and $j$ in benedict-Webb-Rubin-Starling equation of state |
| $L_t$ | Linepack at timestep t [$Mm^3$] |
| $L_0$ | Starting linepack [$Mm^3$] |
| l | Specified length of pipe [m] |
| $m_i, m_j$ | Mole fraction of gas component |
| $n^e$ | Polytropic exponent [1.3] |
| $p$ | Pressure [bar-g] |
| $p_b$ | Compressor station's base pressure [bar-g] |
| $p_m$ | Average pressure of the pipeline [bar-g] |
| $p_s$ | Pressure at standard conditions [bar-g] |
| $p_2$ | Compressor station's discharge pressure [bar-g] |
| $p_1$ | Compressor station's suction pressure [bar-g] |
| $p(0)$ | Pressure at the beginning of pipe [bar-g] |
| $p(l)$ | Pressure at the length $l$ of the pipe [bar-g] |
| Q | Mass flow rate [kg/s] |
| $q$ | Standard volumetric flow rate [$m^3/s$] |
| $q_i^h$ | Standard volumetric flow rate of the $H_2$ injection stream at the injection site[$m^3/s$] |
| $q_i^c$ | Standard volumetric flow rate of the incoming stream at injection site[$m^3/s$] |
| $q_i^o$ | Standard volumetric flow rate of the outgoing stream from the injection site[$m^3/s$] |
| $q_t$ | Standard volumetric flow rate at timestep t [$m^3/s$] |
| $q_0$ | Standard volumetric flow rate at timestep 0 [$m^3/s$] |
| R | Specific gas constant [J/Kg K] |
| $Re$ | Reynolds number of the flow |
| $t$ | Time-step [s] |
| $\theta$ | Temperature [K] |
| $\theta_c$ | Critical temperature [K] |
| $\theta_s$ | Temperature at standard conditions [K] |
| u | Total number of components in the gas mixture |
| V | Volume of gas [$m^3$] |
| v | Gas velocity [m/s] |
| $W$ | Compressor power consumption [W] |
| $x$ | distance along the pipe [m] |
| Z | Gas compressibility factor |
| $Z_S$ | Gas compressibility factor at standard conditions [assumed 0.95] |
| $Z(0)$ | Gas compressibility factor at the beginning of the pipe |
| $Z(l)$ | Gas compressibility factor at the length $l$ of the pipe |
| η | The efficiency of a compressor [assumed 0.8] |
| $\theta$ | Temperature [K] |
| $\rho_s$ | Mass density at standard conditions [$Kg/m^3$] |
| $\rho_m$ | Molar density [$mol/m^3$] |
| $A_0, B_0, C_0, D_0, E_0 \alpha_0, \gamma, a, b, c, \beta$ | Benedict-Webb-Rubin-Starling coefficients. |

[15]. This finding indicates that pipeline networks are the most feasible method for hydrogen transmission within most European countries.

The European Hydrogen Backbone (EHB) report assessed the economic viability of using existing pipeline infrastructure versus constructing new pipelines, finding that repurposing existing natural gas pipelines would cost 33–38 % the cost of building new ones [14]. The European Hydrogen Backbone aims to develop a 53,000 km hydrogen pipeline network across the continent by 2040 [16]. 60 % of these pipelines will be repurposed from existing natural gas infrastructure. Germany and the Netherlands are leading this effort, with plans to repurpose over 10,000 km of pipelines for dedicated hydrogen transmission [17,18].

The UK has also proposed a hydrogen backbone initiative, suggesting that one-third of its pipelines could be repurposed for hydrogen transmission [19]. Like Germany and the Netherlands, gas transmission across Britain is via an extensive network of pipelines designed for delivering natural gas from points of extraction and importation to various demand points [20]. The high-pressure gas transmission network, also known as the National Transmission Network (NTS), has a route length of 7,630 km and is operated by National Gas [20]. The NTS has 24 compressor stations, actively maintaining pressure levels. In this paper, the GB high-pressure gas network was chosen as a case study to understand the impact of $H_2$ gas transmission on high-pressure gas network operation.

The NTS transmits more than 930 TWh of natural gas annually [21] and collects natural gas from geographically far-apart locations. The supply points are gas fields in Scotland and North East England, LNG import sites in South Wales and South East England, storage sites in South West England and interconnectors in North and East England [20]. The NTS delivers natural gas to gas-fired power stations, large industrial sites, and the local distribution zones (LDZ) with lower-pressure gas consumers, such as residential households, scattered across Britain [21].

National Gas plans to utilise the NTS for transmitting $H_2$ [22]. Furthermore, the company plans to repurpose the existing transmission grid to host $H_2$ and natural gas blends (up to 20 % volumetric $H_2$) from 2025 onwards [22]. National Gas plans to repurpose parts of the existing high-pressure gas network to transmit pure $H_2$ gas by repurposing up to one-third of the existing grid to transmit only $H_2$ gas by 2035 [23]. The company also suggests that a pure $H_2$ transmission network could expand nationwide by 2050 [23].

However, $H_2$ and natural gas have different physical characteristics. $H_2$ has a molecular weight 1/8th that of natural gas. The volumetric energy content of $H_2$ gas is 1/3rd of natural gas at standard conditions. These differences in physical characteristics can affect the operation of a natural gas transmission network intending to transport $H_2$.

Numerous research studies has been conducted to investigate the operation of natural gas networks with $H_2$ mixes, which could be grouped into three main topics: 1) operation of compressor stations with $H_2$; 2) linepack fluctuation affected by $H_2$; 3) $H_2$ and natural gas mixture distribution in the network. Table 1 summarise the research papers reviewed.

One of the main operational challenges is compressing $H_2$ gas. As $H_2$ gas has a molecular weight of 1/8th that of methane, centrifugal compressors are much less effective in compressing $H_2$ gas. They must be operated with much higher impeller speeds and additional compression stages [41]. Therefore, reciprocating compressors are more effective for compressing pure $H_2$ gas [41]. Nevertheless, this problem is less severe when $H_2$ gas is injected in lower concentrations, up to 20 % molar concentration of the total mixture [24]. As all the compressors in GB are centrifugal, the FutureGrid project is examining the impact of $H_2$ in the gas mixture on this type of compressor [25].

Many publications have discussed the impact of grid injection of $H_2$ gas on compressor operation. Zabrzeski, L. et al. [26] focused on the

**Table 1**
Summary of the literature review on the operation of gas networks with hydrogen gas mixtures.

| **Topic 1. Operation of compressors with $H_2$ gas.** | | | |
|---|---|---|---|
| **Autour** | **Objective** | **Approach** | **Scale of study** |
| **Adam, P. et al.**[24] | Identifying the most compatible types of compression technology for $H_2$ | Industry survey | European continent |
| **FutureGrid** [25] | To evaluate the capability of the existing fleet of compressors in GB to compress $H_2$ efficiently blends up to 20 % volumetric without compromising operational performance | Physical experiment | A network of pipelines and a centrifugal compressor. |
| **Zabrzeski, L. et al.** [26] | To understand the impact of $H_2$ injection on compressor energy consumption. | Steady state simulation of pipeline and compressor station. | Single pipeline with a single compressor station |
| **Bainer, F. & Kurz, R.**[27] | To assess the impact of $H_2$ injection on energy consumption of centrifugal compressors by focusing on compressor operational maps. | Steady state analysis of a centrifugal compressor station. | Single pipeline with one compressor station |
| **Witek, M. & Uilihoorn, F.**[28] | To analyse the effects of compressor shutdowns and start-ups on gas composition, focusing on the challenges they create in accurately calculating linepack levels in networks with injected $H_2$ gas. | Unsteady-state simulation | Seven pipelines<br>Six injection points. |
| **Topic 2. Impact of $H_2$ gas on network linepack** | | | |
| **Author** | **Objective** | **Approach** | **Scale of study** |
| **Rowley, P. & Wilson, G.**[29] | To quantify the scale of linepack utilisation in GB high-pressure gas network | Numerical observation | GB high-pressure gas network |
| **National Gas**[25] | To quantify the scale of linepack utilisation in GB high-pressure gas network | Numerical observation | GB high-pressure gas network |
| **Wang, C. et al.**[30] | To investigate the impact of $H_2$ injection on pressure levels and linepack in the gas network. | Unsteady-state analysis | Eight pipelines with three compressor stations and three injection points |
| **Wesselink, O. et al.** [31] | To investigate the link between $H_2$ injection, linepack levels, and pipeline deterioration in gas networks. | Unsteady-state analysis<br>Defect growth calculation model | Model of Dutch high-pressure gas network |
| **Wu, C. et al.** [32] | To Propose a methodology for studying the impacts of time-varying hydrogen injection on linepack, affecting optimal dispatch of coupled electricity and gas networks. | Optimisation<br>Quasi-Steady state | 12 node gas network model |
| **Jiang Y et al.** [33] | To Propose a methodology for studying the impacts of time-varying hydrogen injection on linepack, affecting optimal dispatch of coupled electricity and gas networks. | Optimisation<br>Unsteady-state | 20-node gas network model |
| **Topic 3. Variations of H2 gas volume after injection into pipeline** | | | |
| **Author** | **Objective** | **Approach** | **Scale of study** |
| **Fernandes. L. et al** [34] | To identify the impact of the shape of the H2 gas injector on the mixing of $H_2$ and natural gas in the pipelines. | Computational fluid dynamics | Single pipeline |
| **Khabbazi. A. et al.** [35] | To identify the impact of flow momentum on the mixing of $H_2$ and natural gas in the pipeline<br>To understand the impact of the angle of $H_2$ injection on the mixing of $H_2$ and natural gas in the pipeline | Computational fluid dynamics | Single pipeline |
| **Guandalini, G. et al.**[36] | To develop and apply a model that simulates the unsteady operation of a gas grid incorporating the direct injection of $H_2$, to assess compliance with composition and quality constraints in dynamic scenarios. | Unsteady-state simulation | Single pipeline |
| **Zhou, D. et al.** [37] | Investigated the impact of $H_2$ injection on pressure losses in the gas network. | Optimisation<br>Steady-State | 10-node model of Hunai & Hubei provinces in China |
| **Zhang, Z. et al.**[38] | To Improve the computational methods for simulating the injection and the mixing of $H_2$ and natural gas in the high-pressure gas network. | Unsteady-state simulation | 20-node model of the Belgian gas network<br>Four $H_2$ injection points. |
| **Ekhtiari, A. et al.** [39] | To evaluate the feasibility and impact of integrating power-to-H2 (P2H) systems into the Irish gas transmission network, utilising $H_2$ produced from curtailed renewable electricity.<br>Aims to analyse key gas network parameters, including pipeline pressure drop, flowrate,, composition, and calorific content, under varying wind speeds and gas demands over 24 h | Unsteady-state simulation | 23-node model of the Irish high-pressure gas network.<br>3 $H_2$ injection points.<br>2 compressor stations. |
| **Saedi, I. et al.**[40] | To present a novel integrated electricity and gas system model with green $H_2$ injections and gas composition tracking.<br>To identify the maximum number of renewable energy sources to be integrated while maintaining $H_2$ levels in the gas network can remain at 20 % volumetric. | Steady-state optimisation model | 48-node model of network.<br>27 $H_2$ injection points.<br>10 compressor stations<br>7 pressure regulators. |

impact of $H_2$ gas injection on the performance of reciprocating compressors. They highlighted that injection of 5 % $H_2$ resulted in 10 % decrease of theoretical energy required for running the compressors.

Bainier, F. & Kurz, R. [27] investigated the impact of grid $H_2$ injection on centrifugal compressors. The authors highlighted that the operation of centrifugal compressors is more energy-intensive with increasing $H_2$ content in the gas mix. In addition, Bainier, F. & Kurz, R. emphasised that increasing $H_2$ concentration beyond 20 % leads to an exponential increase in centrifugal compressor energy demand.

Compressor operation can also change the network's $H_2$ content. A paper by Witek, M. & Uilhoorn, F. [28] observed that sudden compressor shutdowns in a network with larger $H_2$ content leads to faster fluctuations in pressure and linepack levels. A phenomenon that could pose a challenge in managing rapid events in the gas network.

Linepack, the gas network's capacity to store gas, is a crucial feature that shields the network from unexpected demand surges. For the GB gas network, linepack is one of the most frequently utilised attributes. The extent of annual linepack utilisation in GB is highlighted by Rowley & Wilson [42] and documented by National Gas [42]. The low energy density of $H_2$ gas causes changes to this attribute and as the $H_2$ gas has a heating value per unit volume 1/3rd that of natural gas at standard conditions. As demonstrated by Wang, C. et al. [30], as the percentage of $H_2$ in the network increases, the pressures in the network need to increase to keep the same level of linepack in energy terms. A paper by Wesselink, O. et al. [31] highlighted that in a gas network with $H_2$ gas injections, an increase in pressure and consequently linepack level will induce pipeline deterioration, and linepack levels need to be optimised to keep this phenomenon to a minimum. Papers by Wu, C. et al. [32] and Jiang, Y. et al. [33] revealed how linepack levels change due to fluctuations in renewable-generated $H_2$ gas injected into the gas network.

Many research papers have comprehensively examined the operation of gas networks with hydrogen injection. When $H_2$ gas and natural gas mix, the gas heating value will change. As the heating value of the mixed gas decreases by injecting more hydrogen to the network, to supply the same amount of energy, the volumetric flow of the mixed gas should increase which consequently affect pressure, linepack levels, and compressor stations' energy consumption.

Only a small number of papers have studied the regime under which $H_2$ gas and natural gas mix in pipelines in real gas networks. Work by Fernandes. L. et al.[34] and Khabbazi, A. et al. [35] investigated the effect of $H_2$ injection method on $H_2$ and natural gas mixture in the pipeline computational fluid dynamics in the Italian gas network. A paper focusing on a mixture along the pipe is by Guandalini, G. et al. [27], where $H_2$ gas is injected midway along a single pipeline. A paper by Zhou, D. et al [37] investigated the impact of $H_2$ injection on pressure losses in the gas network. The authors used a 10-node representation of Henan and Hubei gas network. Zhang, Z. et al. [38] investigated how $H_2$ gas mixes in a 20-node representation of the Belgian gas network using 4 $H_2$ injection points. Their focus was on improving the methodology used to simulate $H_2$ and natural gas mixture. The most extensive study is by Ekhtiari, A. et al. [39] using a 23-node representation of the Irish high-pressure gas network. The findings of all the studies pointed out that $H_2$ gas and natural gas do not mix homogeneously in networks. Some papers have attempted to mitigate the inhomogeneous mixture of hydrogen and natural gas in pipelines by optimising $H_2$ injection rates during the day. Saedi, I. et al. [40] developed an optimisation model that finds the optimal gas flow for maintaining a consistent $H_2$ content in parts of the Australian gas network. The achievements of these research papers are significant; however, the problem of the $H_2$ gas mixture in gas networks is highly dependent on the structure of the gas network. Moreover, the studies conducted on the Irish, Belgian, and Australian gas networks do not identify specific challenges that the GB gas network is likely to face with this issue.

Since the GB gas network is amongst the most complex gas networks, it is vital to develop a highly granulated model and study the operation of compressor stations, the fluctuations of linepack levels and, most importantly, study the $H_2$ and natural gas mixture in every location specific to the GB gas network. The specific research questions related to the operation of the GB gas and hydrogen networks are:A. How would increasing the share of $H_2$ gas in the gas network affect operational attributes of the high-pressure gas network, such as pressure levels, linepack and compressor energy consumption?

B. Assuming that the $H_2$ gas supply will be geographically dispersed across the network, how does the location of $H_2$ injection sites affect the volumetric percentage of $H_2$ gas across the network?

To address the above questions, a simulation model of the GB high-pressure gas network was developed using Synergi Gas 4.9.4. software. The model has a high granularity, with 294 nodes, 356 pipes, and 24 compressor stations. Unsteady-state analysis was chosen to investigate the operation of compressor stations and the linepack throughout a selected day. Component tracing analysis has been used to simulate the $H_2$ and natural gas mixture.

Five case studies were conducted: one to represent the existing natural gas network in Great Britain on a typical winter day in 2018, one to represent the operation of gas network in the year 2035 with NG 2035, another to represent a gas network in 2035 with 20 % volumetric hydrogen injection from 8 gas entry points using the hydrogen steam reformation process (SMR), another to represent a gas network in 2035 with 20 % volumetric hydrogen injection from 28 injection points co-located with wind farms dispersed across GB, and finally, a case study representing the operation of the same gas network with 100 % hydrogen in the year 2050.

The paper is organised as follows: Section two describes the methodology for simulating the GB high-pressure gas network, showcasing the high-pressure gas network model developed in Synergi 4.9.4. Section three discusses the five case studies used to analyse the operation of the high-pressure gas network with different levels of $H_2$ gas. Section four shows the simulation results and presents discussions, and finally section five provides the conclusions. The paper also discusses the accuracy of the GB high-pressure gas network model in Appendix I. In Appendix II, the paper provides a sensitivity analysis, examining the dependence of operational parameters of pressure and linepack on $H_2$ content in the network.

## 2. Unsteady state analysis of the gas network

The equations in section 2.1- 2.5 are directly from Synergi Gas 4.9.4. Manual [43].

### 2.1. Flow along a pipe

The equations for the conservation of mass and momentum along a single straight pipe, neglecting the altitude of the pipe, are:

$$\frac{\partial}{\partial x}(\rho v) + \frac{\partial p}{\partial t} = 0 \tag{1}$$

$$\rho\frac{dv}{dt} = -\frac{\partial p}{\partial x} + F \tag{2}$$

Equation (3) describes the absolute derivative in a moving control boundary as the partial derivative of both time ($\frac{\partial}{\partial t}$) and motion of the control boundary ($v\frac{\partial}{\partial x}$):

$$\frac{d}{dt} = \frac{\partial}{\partial t} + v\frac{\partial}{\partial x} \tag{3}$$

where ρ, v and p are the density, velocity and pressure of the gas, respectively, x is the distance along the pipe and t is the time.

The mass flow rate Q along the pipe is given by:

$$Q = \rho A v \tag{4}$$

where A is the cross-sectional area of the pipe. The frictional force, F, is given by:

$$F = -\frac{k_F|q|^{a-1}q}{2|p|} \tag{5}$$

where q is the standard volumetric flowrate along the pipe, $k_F$ is the friction factor of the pipe and a is the gas flow exponent.

The friction factor of the pipe is calculated using Colebrook equation:

$$\frac{1}{\sqrt{k_F}} = -2\log_{10}\left[\left(\frac{\epsilon/d}{3.7}\right) + \frac{2.51}{\mathrm{Re}\sqrt{k_F}}\right] \tag{6}$$

where ∊ is the roughness of pipe, assumed to be 0.067 mm [44] and Re is the Reynolds number of flow. The standard volume is the volume that a given mass of gas would occupy at standard conditions. The standard volume flow rate is therefore related to the mass flow rate by:

$$q = \frac{Q}{\rho_s} \tag{7}$$

where $\rho_s$ is the density at standard conditions.

For a fixed mass of gas:

$$\frac{pV}{Z\theta} = \text{constant} \tag{8}$$

where V is the volume of the gas, θ is the temperature and Z is the compressibility. From this, a relationship between pressure and density is obtained:

$$p = \frac{\rho}{\rho_s}\frac{Z\theta}{Z_S\theta_S}p_s \tag{9}$$

where $\theta_S$ and $p_s$ are the standard temperature and pressure, and $Z_S$ is the compressibility at the standard conditions.

Considering the long-term variation in pressure, the effect of the momentum on the gas will be small and the frictional forces are expected to dominate.

Thus, the term representing momentum $\rho\frac{dv}{dt}$ in Equation (2) is neglected. The conservation equations are thus transformed:

$$\frac{\partial}{\partial x}(p|p|) + k_F|q|^{a-1}q = 0 \tag{10}$$

$$\frac{1}{A}\frac{\partial q}{\partial x} + \frac{Z_s\theta_s}{p_s}\frac{\partial}{\partial t}\left(\frac{p}{Z\theta}\right) = 0 \tag{11}$$

Assuming that the temperature of the gas is constant over time, Equation (11) is simplified:

$$\frac{1}{A}\frac{\partial q}{\partial x} + \frac{Z_s\theta_s}{p_s\theta}\frac{\partial}{\partial t}\left(\frac{p}{Z}\right) = 0 \tag{12}$$

### 2.2. Spatial discretisation

Using Taylor's expansion method, the spatial discretisation of flow along a pipeline is given in equation (13). This formula defines the relationship between pressure drop and flow along a pipeline:

$$q - q(0) = -\frac{1}{2}l\frac{AZ_S\theta_S}{p_s\theta}\left[\frac{\partial}{\partial t}\left(\frac{p(0)}{Z(0)}\right) + \frac{1}{3}\left(\frac{\partial}{\partial t}\left(\frac{p(l)}{Z(l)}\right) - \frac{\partial}{\partial t}\left(\frac{p(0)}{Z(0)}\right)\right)\right] + \frac{1}{24}l^2\frac{(a-1)}{q}\left(\frac{AZ_S\theta_s}{p_s\theta}\frac{\partial}{\partial t}\left(\frac{p}{Z}\right)\right)^2 \tag{13}$$

where p(0) and Z(0) are pressure and compressibility factors at the beginning of the pipe and p(l) and Z(l) are pressure and compressibility factors at the length l of the pipe.

### 2.3. Linepack

Linepack in the pipeline at time t is simulated as in equation (14):

$$L_t = L_0 + \int_0^t (q - q(0))dt \tag{14}$$

where $L_0$ is the pipeline linepack at the beginning of the simulation, which is calculated using steady-state conditions. This is also referred to as the starting linepack:

$$L_0 = \frac{p_m A l}{p_s Z R \theta_S} \tag{15}$$

where A is the cross-sectional area of the pipe and l is the length of the pipe and $p_m$ is the average pressure of the pipeline.

### 2.4. Compressor power

The relationship between compressor energy consumption, gas flow in the compressor, and suction and discharge pressures was modelled using Equation (16).

$$W = \frac{P_b.q.n^e}{\eta(n-1)}\left[\left(\frac{p_2}{p_1}\right)^{\frac{n-1}{n}} - 1\right] \tag{16}$$

$P_b$ is set to be 1 bar-g.

### 2.5. Component tracing analysis

Two different gas streams were defined, 100 % $H_2$ gas and GB natural gas. The 100 % $H_2$ gas only contains molecular $H_2$ gas, and the GB natural gas was defined by five main components, as shown in Table 2:

Synergi Gas recommends the Starling modification of Benedict-Webb-Rubin (BWRS) to simulate the composition of mixed gas in each node during the simulation. The BWRS equation of state is presented in equation (17):

$$p = \rho_m R\theta + \left(B_0R\theta - A_0 - \frac{C_0}{\theta^2} + \frac{D_0}{\theta^3} + \frac{E_0}{\theta^4}\right)\rho_m^2 + \left(bR\theta - a - \frac{\beta}{\theta}\right)\rho_m^3 + \alpha\left(a + \frac{d}{\theta}\right)\rho_m^6 + \frac{c\rho_m^2}{\theta^2}(1 + \gamma\rho_m^2)\exp(-\gamma\rho_m^2) \tag{17}$$

where the 10 coefficients can be evaluated from equations (18) to (28):

$$A_0 = \sum_i^u\sum_j^u m_i m_j A_{0i}^{\frac{1}{2}} A_{0j}^{\frac{1}{2}}(1 - k_{ij}) \tag{18}$$

$$B_0 = \sum_i^u m_i B_{0i} \tag{19}$$

$$C_0 = \sum_i^u\sum_j^u m_i m_j C_{0i}^{\frac{1}{2}} C_{0j}^{\frac{1}{2}}(1 - k_{ij})^3 \tag{20}$$

$$D_0 = \sum_i^u\sum_j^u m_i m_j D_{0i}^{\frac{1}{2}} D_{0j}^{\frac{1}{2}}(1 - k_{ij})^4 \tag{21}$$

$$E_0 = \sum_i^u\sum_j^u m_i m_j E_{0i}^{\frac{1}{2}} E_{0j}^{\frac{1}{2}}(1 - k_{ij})^5 \tag{22}$$

$$\alpha = \left[\sum_i^u m_i\alpha_i^{\frac{1}{3}}\right]^3 \tag{23}$$

$$\gamma = \left[\sum_i^u m_i\gamma_i^{\frac{1}{3}}\right]^3 \tag{24}$$

$$a = \left[\sum_i^u m_i a_i^{\frac{1}{3}}\right]^3 \tag{25}$$

**Table 2**
Assumed components of natural gas.

| Component | Molecular Percentage % |
|---|---|
| Methane | 93 |
| Ethane | 3 |
| Propane | 2.1 |
| Nitrogen | 1.6 |
| Carbon dioxide | 0.3 |

$$b = \left[\sum_{i}^{u} m_i b_i^{\frac{1}{3}}\right]^3 \tag{26}$$

$$c = \left[\sum_{i}^{u} m_i bc_i^{\frac{1}{3}}\right]^3 \tag{27}$$

$$\beta = \left[\sum_{i}^{u} m_i \beta_i^{\frac{1}{3}}\right]^3 \tag{28}$$

$m_i$ and $m_j$ are the mole fraction of the components $i$ and $j$ in the mixture, respectively. Furthermore, $k_{ij}$ is the interaction coefficient of the components $i$ and $j$ in the mixture. The $k_{ij}$ values for the components are listed in Table 3. These values are as provided in Synergi manual, and can also be found in work by Lielmezs, J. [45]:

*$H_2$ injection method*

In GB, National Gas has conducted physical tests on all types of assets used in the high-pressure network. The results of these tests have been published in the FutureGrid Phase 1 closure report and state that the presence of H2 up to 20 % volumetric in the network is safe[46] Therefore, the 20 % volumetric limit is also adopted for the model in this study.

To implement this ratio, each injection site is modelled as follows. At each injection site, there are three gas streams: 1) $H_2$ injection stream $q_i^h$. 2) Incoming stream $q_i^c$. 3) Outgoing stream $q_i^o$ .This is described in Fig. 1.

At each node of the network, gas flow balance equation applies, dictating that the volumetric flow of gas incoming and outgoing a node are equal. At the $H_2$ injection node, the relationship between the outgoing stream $q_i^o$, incoming steam $q_i^c$ and hydrogen injection stream $q_i^h$ is therefore defined as:

$$q_i^o = q_i^h + q_i^c \tag{29}$$

At the injection node, it was ensured that the hydrogen injection stream $q_i^h$ constitutes to only 20 % volumetric of the outgoing stream $q_i^o$:

$$\frac{q_i^h}{q_i^h + q_i^c} = 20\% \tag{30}$$

Therefore the volume of $H_2$ injection stream $q_i^h$ was set to ¼ of the amount of the incoming gas stream $q_i^c$ at all time steps:

$$q_i^h = \frac{1}{4} q_i^c \tag{31}$$

Note that this does not factor $H_2$ that is already in the incoming stream.

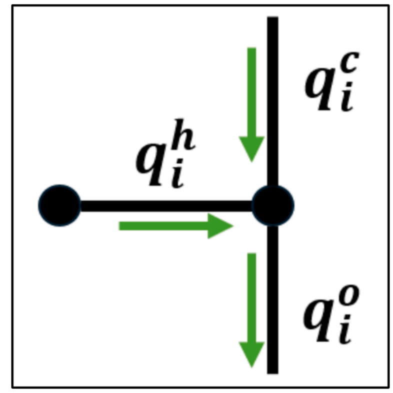


**Fig. 1.** Schematic describing $H_2$ injection nodes and pipes.

## 3. The high-pressure gas network model

The transient model of the gas network was developed using data taken from National Gas [20,47–51]. The model has 284 nodes, consisting of nine supply points, 13 nodes representing industries directly connected to the high-pressure gas network, 34 nodes representing gas-fired power stations, and 78 nodes representing demands from lower-pressure gas networks, such as Local distribution zones (LDZ) connected to the high-pressure network. The rest of the nodes are junction points where pipelines connect. The network is divided into 12 zones and six regions. Fig. 2 displays a map of the developed model of the high-pressure gas network. The colour-key in Fig. 2 corresponds to the linepack zones in the high-pressure gas network model. The compressor stations in Fig. 2 have reference numbers and Table 4 lists the names of the compressor stations corresponding to the references.

In Synergi 4.9.4. supply and demand levels are defined in energy terms. The model calculates demand in volumetric terms, the pressure at each node in the network, the linepack of each pipe, compressor energy consumption and gas composition in every node at each time step.

Synergi Gas 4.9.4 software conducts Unsteady-state simulation with component tracing analysis simultaneously. Demand and supply values were taken from the National Gas Database. [51]. The model's assumptions are summarised in Table 5.

### 3.1. Description of case studies

Five case studies were analysed to demonstrate the operation of the high-pressure gas network on a winter day in 2018, 2035 and 2050. Table 6 provides an overview of the case studies.

The gas supply and demand in the five case studies are shown in Fig. 3. In the NG 2018 case, most of the gas is supplied from Scotland and the North East region, while in the other case studies, the South East region supplies most of the gas. The gas supply and demand profiles were set following National Gas' predictions.

The energy demand in the 20 % Centralised and the 20 % Distributed Injection cases is 58 % that of the NG 2018. This reduction represents National Gas' projections [3] of gas demand for 2035 and 2050. The two

**Table 3**
The interaction coefficient $k_{ij}$ between different gases used in this study.

| | Methane | Ethane | Propane | Hydrogen | Nitrogen | Carbon-dioxide |
|---|---|---|---|---|---|---|
| **Methane** | 0 | 0.01 | 0.023 | 0 | 0.025 | 0.05 |
| **Ethane** | | 0 | 0.0031 | 0 | 0.07 | 0.048 |
| **Propane** | | | 0 | 0 | 0.1 | 0.045 |
| **Hydrogen** | | | | 0 | 0 | 0 |
| **Nitrogen** | | | | | 0 | 0 |

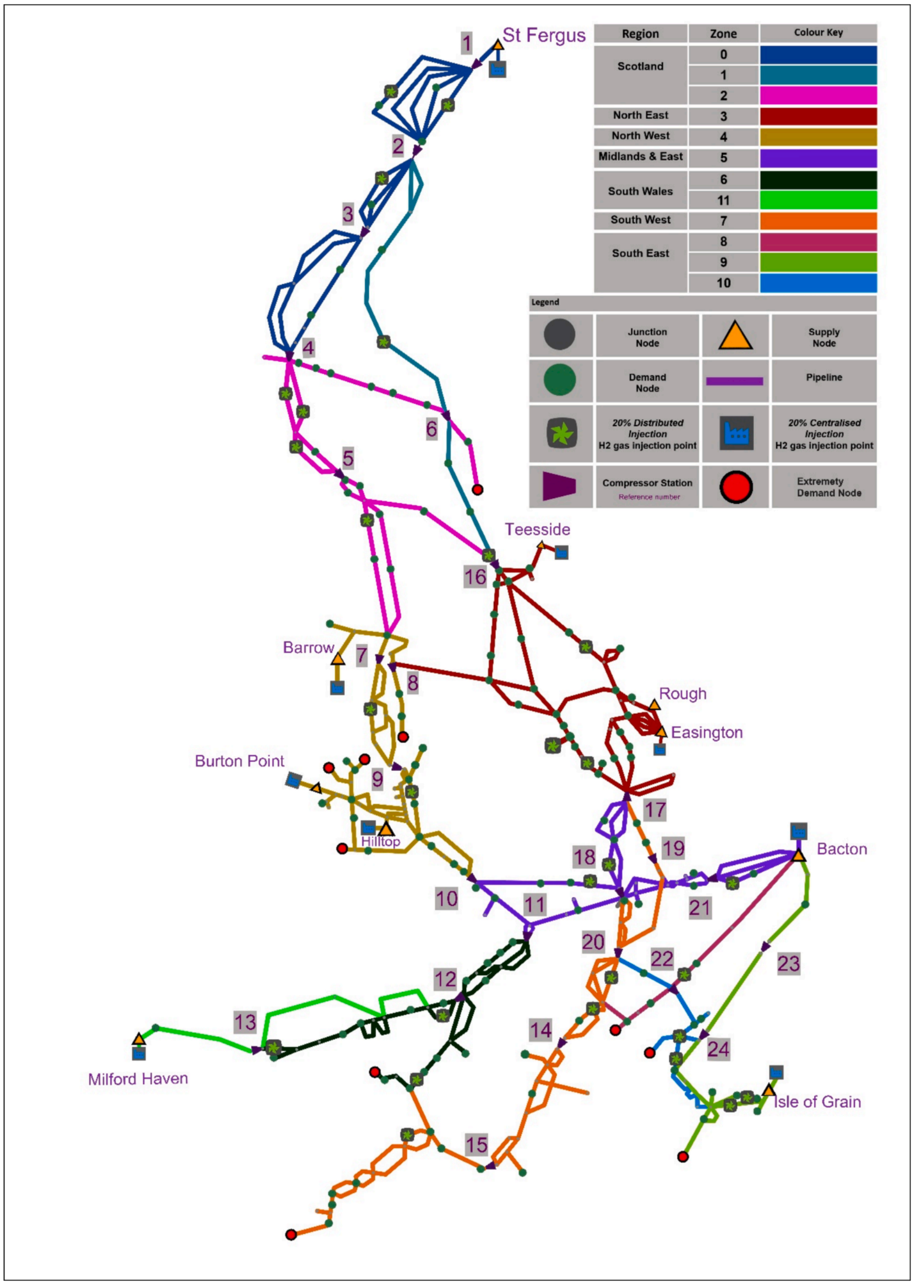


**Fig. 2.** Schematic of the NTS model.

**Table 4**
Compressor stations in NTS map in Fig. 2.

| Reference Number | Compressor | Reference Number | Compressor |
|---|---|---|---|
| 1 | **St Fergus** | 13 | **Felindre** |
| 2 | **Aberdeen** | 14 | **Aylesbury** |
| 3 | **Kirriemuir** | 15 | **Lockerley** |
| 4 | **Avonbridge** | 16 | **Bishop Auckland** |
| 5 | **Moffat** | 17 | **Hatton** |
| 6 | **Wooler** | 18 | **Peterborough** |
| 7 | **Carnforth** | 19 | **Wisbech** |
| 8 | **Nether Kellet** | 20 | **Huntingdon** |
| 9 | **Warrington** | 21 | **King's Lynn** |
| 10 | **Alrewas** | 22 | **Cambridge** |
| 11 | **Churchover** | 23 | **Diss** |
| 12 | **Wormington** | 24 | **Chelmsford** |

**Table 5**
Summary of assumptions in the model.

| | Inputs to model | Outputs from model |
|---|---|---|
| Supply Node | Gas supply in energy terms (GWh) | Pressure level (bar-g) |
| | Pressure level at initial condition (t = 0) | % Of each gas composition |
| Demand Node | Gas demand in energy terms (GWh) | Pressure level (bar-g) |
| | Pressure level at initial condition (t = 0) | % Of each gas in the node |
| | | Gas demand in volumetric terms ($Mm^3$/h) |
| Junction Node | Zero demand/zero supply | – |
| Pipeline | Pipeline length (km) and diameter (m), and absolute roughness (mm) | Linepack in volumetric terms ($Mm^3$) and in energy terms (GWh) |
| Compressor Station | Installed power (MW) | Energy consumption (MWh) |
| | Minimum inlet pressure limit (bar-g) | Inlet and outlet pressure levels |
| | Maximum outlet pressure limit (bar-g) | |
| | Set pressure (either on the inlet or outlet) | |

**Table 6**
Overview of the Case Study Assumptions.

| **Case Study** | **Year** | **Time-step** | **Length of simulation** | **Supply (GWh)** | | |
|---|---|---|---|---|---|---|
| | | | | **Natural Gas** | **Wind-generated $H_2$ gas** | **SMR-generated $H_2$ gas** |
| NG 2018 | 2018 | 10-minute | 24-hours | 2913.5 | — | — |
| NG 2035 | 2035 | 10-minute | 24-hours | 1690.3 | — | — |
| 20 % Centralised Injection | 2035 | 10-minute | 24-hours | 1572 | — | 118.3 |
| 20 % Distributed Injection | 2035 | 10-minute | 24-hours | 1572 | 118.3 | — |
| 100 % $H_2$ | 2050 | 10-minute | 24-hours | — | — | 1690.3 |

**Table 7**
Description of compressor station setup in the NG 2018 case.

| Compressors | Purpose | Set-Pressure (bar-g) |
|---|---|---|
| St Fergus | • Boosting pressures at St Fergus Terminal | • 40 @ Inlet |
| Aberdeen | • Directing flow from St Fergus towards Scotland and the North of England<br>• Keeping pressures below 65 bar-g between St-Fergus and Aberdeen | • 55 @ Outlet |
| Nether Kellet | • Supporting pressures at network extremities, Blackrod and Blackburn | • 75 @ Outlet |
| Hatton | • Supporting gas flowing from the North East to the South of England | • 75 @ Outlet |
| King's Lynn | • Supporting gas flowing from the Bacton terminal towards the Midlands<br>• Keeping Bacton pressures below 75 bar-g | • 75 @ Outlet |
| Huntingdon | • Supporting gas flowing from the Midlands towards the South West | • 75 @ Outlet |

**Table 8**
Description of compressor station setup in the NG 2035, 20% Centralised Injection and 20% Distributed Injection case studies (all these case studies envisage the network in year 2025).

| Compressors | Purpose | Set pressure (bar-g) |
|---|---|---|
| St Fergus | • Same as the NG 2018 case | 40 @ Inlet |
| Aberdeen | • Same as the NG 2018 case | 55 @ Inlet |
| Nether Kellet | • Same as the NG 2018 case | 70 @ Outlet |
| Diss | • Supporting flow of gas from Bacton | 55 @ Inlet |
| Alrewas | • Used to direct flows from the Midlands towards the North West. | 55 @ Inlet |
| Churchover | • Used to direct flows from the Midlands towards South Wales | 58 @ Inlet |
| King's Lynn | • Same as the NG 2018 case | 55 @Inlet |
| Huntingdon | • Same as the NG 2018 case | 55 @Inlet |

**Table 9**
Description of compressor station setup in the 100% $H_2$ case study.

| Compressors | Purpose | Set pressure (bar-g) |
|---|---|---|
| St Fergus | • Same as the NG 2018 case | 40 @ Inlet |
| Aberdeen | • Same as the NG 2018 case | 55 @ Inlet |
| Nether Kellet | • Same as the NG 2018 case | 65 @ Outlet |
| Diss | • Supporting flow of gas from Bacton | 55 @ Inlet |
| Alrewas | • Used to direct flows from the Midlands towards the North West. | 50 @ Inlet |
| King's Lynn | • Same as the NG 2018 case | 55 @Inlet |
| Huntingdon | • Same as the NG 2018 case | 55 @Inlet |
| Lockerley | • Supporting pressures at extremities in southwest England | 70 @Outlet |
| Felindre | • Supporting flow of gas from Milford Haven | 50 @ Inlet |

cases in which hydrogen is injected into natural gas have the same gas supply and demand. Note that the slight difference between supply levels in injection cases is due to the varying location of $H_2$ injection points between the two cases.

The energy demand in the 100 % $H_2$ case is the same as in both the 20 % Centralised and the Distributed injection cases; however, as $H_2$ has a lower energy density, the volumetric flow rate of the 100 % $H_2$ case study increases significantly compared to both 20 % Centralised and Distributed Injection cases.

### 3.1.1. Case 1: NG 2018

The GN 2018 case represents a typical winter day in 2018 when the network transports natural gas. The year 2018 was chosen since it was before the COVID-19 pandemic, which affected GB gas consumption between 2019 and 2021. The winters after the COVID-19 pandemic could not be selected because the Russia-Ukraine conflict also affected gas demand and supply patterns. The gas demand and supply of the NG 2018 case are shown in Fig. 4, demonstrating the various demand patterns of sectors for 24 h.

In 2018, St Fergus supply terminal supplied most of the gas to the NTS. Therefore, in the NG 2018 case, compressor stations in Scotland and North England were set to support gas flow from Scotland to the South of England via the North East region. [48].

The pressure levels in the network should always remain within a range to satisfy commercial and safety requirements. The upper bound of this range varies in each region depending on the maximum operating pressures of the pipelines, which is between 70 – 90 bar-g [47]. The minimum of this range depends on the compressor's minimum inlet pressure, which is 40 bar-g [48]. Compressors used in the NG 2018 case are described in Table 7.

### 3.1.2. Case 2:NG 2035

The case depicts the operation of the GB natural gas network in 2035 without any H2 gas. In the NG 2035 case, supply from St-Fergus in Scotland declines, and Bacton becomes the leading gas terminal in the East of England. This means that the flow of gas changes direction from East to North.

To simulate this scenario, the supply of gas has been changed, as seen in Fig. 3. The compressors were set to move gas away from the East towards neighbouring regions. Table 8 describes the compressors used in this case study.

### 3.1.3. Case 3: 20 % centralised injection

The 20 % Centralised Injection study investigated the effects of injecting $H_2$ gas into the grid on a typical winter day in 2035. $H_2$ is injected from the same points as the natural gas supply terminals. The $H_2$ injected into the grid is assumed to be generated with SMR (blue $H_2$ gas). It is assumed that at each injection point, 20 % $H_2$ gas will be injected into the natural gas stream. Because the natural gas supply is assumed to be constant within one hour, the $H_2$ injection is also constant within one hour. The total $H_2$ gas injected is 35 $Mm^3/d$.

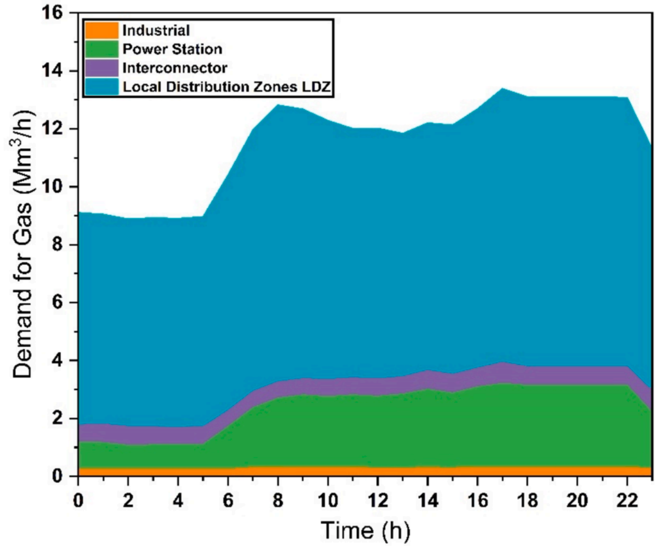


**Fig. 4.** Demand for gas by sectors in the NG 2018 case.

The gas flow is the same as in the NG 2035 case, so the compressors used are also the same, as described in Table 8.

### 3.1.4. Case 4: 20 % distributed injection

This 20 % Distributed Injection study investigates the effects of injecting $H_2$ gas from wind generation across GB on a typical winter day in 2035, with 28 $H_2$ gas injection points close to the wind farms across GB. The location of the injection node was determined using the Future Energy Scenarios regional data generated by National Grid: ESO. [6]. The location of each injection point is marked in Fig. 2. As in the Centralised Injection case, the hourly injection rate is 20 % of the volumetric stream flow rate. The hydrogen gas injected into each region is shown in Fig. 5.

### 3.1.5. Case 5: 100 % $H_2$

The 100 % $H_2$ case represents a typical winter day in 2050 when the

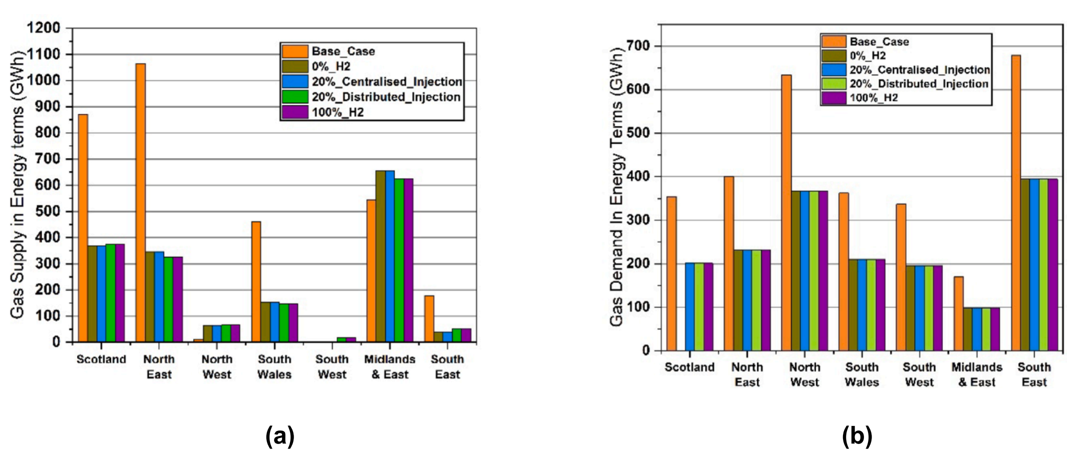


**Fig. 3.** Daily gas supply and demand, (a) regional supply and (b) regional demand.

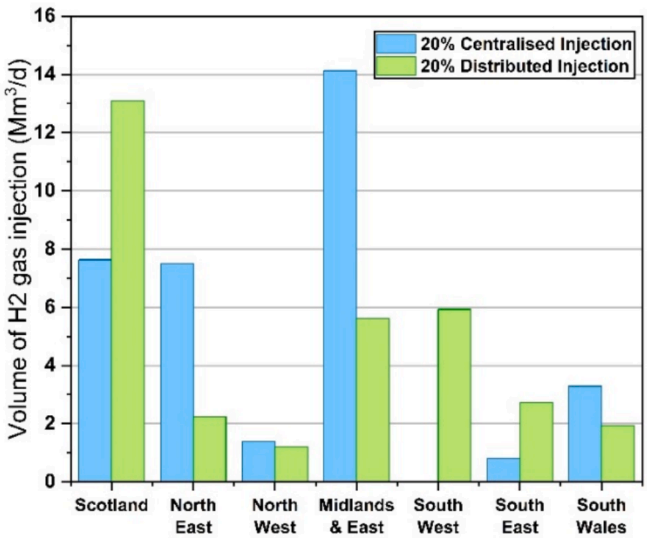


**Fig. 5.** The volume of $H_2$ gas injected into each region.

network only transports $H_2$ gas. 1690.3 GWh of $H_2$ generated by methane reformation with carbon capture and storage.

The compressor settings are different from the rest of the cases because the gas flow volume is anticipated to be much larger than in other cases. The compressors used in this case study are described in Table 9.

In the 100 % $H_2$ case, the compressor energy consumption is not limited to the existing compressor capacity. This was done to measure the extra energy required to compress pure $H_2$.

## 4. Results and discussion

The results of the case studies are presented in the following section, including 1) the operation of the gas network and 2) $H_2$ gas composition across the network. The high-pressure gas network operation was investigated in three aspects: pressure levels, linepack levels and compressor energy consumption.

To validate the model and verify the robustness of the findings, the NG 2018 case simulation results were compared with real operational data from the 2018 winter season. This comparison is presented in Appendix I. Furthermore, a sensitivity analysis was conducted, investigating the impact of $H_2$ injection on pressure and linepack levels. The sensitivity analysis is presented in Appendix II.

### 4.1. Operation of the gas network with $H_2$ gas

#### 4.1.1. Pressure levels

Fig. 6 shows the maximum pressures of supply points and extremities against their minimum pressures experienced during the 24-hour simulation.

Here, extremities are the nodes at the far ends of the high-pressure network at a considerable distance from the supply points. One node in Scotland, four nodes in North West England, three nodes in South East England, one in South West England, and one in South Wales have been chosen as extremities node. These demand nodes are marked on the map on Fig. 1.

The axes in Fig. 6 have a data rug that shows how clustered or dispersed the pressure levels are. The pressure points are colour-mapped, and their colour corresponds to the daily gas flow in each node.

As gas demand and supply in energy terms are inputs to the model, their volumetric flow is an output from the model, calculated based on the gas composition at each timestep.

Fig. 6 (a) shows that pressures in the NG 2018 case are distributed with maximums ranging between 40–71.5 bar-g and minimums between 40–69.5 bar-g. As seen in Fig. 6 (a-1), in the NG 2035 case, the range changes and the maximum pressure levels vary between 40–67.5 bar-g and the minimum pressure levels vary between 40–65 bar-g,. Fig. 6 (b) shows that in the 20 % Centralised Injection, the maximum pressures range between 40–68 bar-g, and the minimum pressures also range between 40–67.5 bar-g. Fig. 6 (c) shows that the 20 % Distributed Injection also has a similar pressure range with maximums between 40–70 bar-g and minimums between 40–68 bar-g. Fig. 6 (d) shows that the 100 % $H_2$ case has a similar pressure range with maximums between 40–71 bar-g and minimums between 40–65 bar-g.

The pressure levels in the NG 2018 case and the 100 % $H_2$ case are more dispersed than in NG 2035, 20 % Centralised and the 20 % Distributed Injection cases, as shown in the Fig. 6 graphs. The standard deviation of pressure levels presented in Fig. 6 was calculated and compared to quantify this dispersion. The NG 2018 case and the 100 % $H_2$ case have pressure levels with a 5.9 and 5.8 bar-g standard deviation. The NG 2035, 20 % Centralised, and 20 % Distributed Injection cases have similar pressure levels ranging between 4.1–4.3 bar-g.

The colourmaps in Fig. 6 show that as the H2 content in the gas network increases, the volumetric flow of demand and supply nodes also increases. Furthermore, the colourmap of nodes in Fig. 6 shows that the nodes in the NG 2018 case and the 100 % $H_2$ case experience higher volumetric flow rates than the NG 2035, 20 % Centralised and 20 % Distributed Injection cases. This is especially clear for the NG 2018 case and the 100 % $H_2$ case, each of which has fewer than 2 of the extremities with a daily flow rate of less than 2 $Mm^3/d$, while for the other three cases, there are 7 of the extremities with such low flow rates.

#### 4.1.2. Linepack levels

Fig. 7 demonstrates the total network linepack for every simulation hour. Fig. 7 (a) shows linepack in energy terms and Fig. 7 (b) in volumetric terms.

As shown in Fig. 7(a) the volumetric starting linepack of the NG 2018 case, NG 2035, 20 % Centralised Injection and 20 % Distributed Injection cases are extremely similar, ranging between 346.9–350 $Mm^3$. However, the volumetric starting linepack of 100 % $H_2$ case is much lower than other cases, at 312 $Mm^3$.

Comparing the volumetric starting linepack of the NG 2035 case with the 100 % case, despite the rise in volumetric flows in the 100 % $H_2$ case, the starting linepack has reduced. This demonstrates that demand and supply levels do not correlate with the starting level of the linepack in the network.

As seen in Fig. 7(b), the starting linepack in energy terms is distinct from the volumetric starting linepack levels. The NG 2018 case and NG 2035 case have close starting linepack levels of 3865.2 and 3949.5 GWh. Also, the 20 % Centralised Injection and 20 % Distributed Injection cases have similar starting linepack levels in energy terms, 3369 and 3431 GWh The 100 % $H_2$ case has the lowest starting linepack in energy terms, 997.3 GWh.

This trend clearly shows that with the introduction of $H_2$ to the network, the linepack in energy terms decreases.

Fig. 7(a) also shows that fluctuations of volumetric linepack levels in the 100 % $H_2$ case are more significant than in the other cases. For example, from the hours 0 to 6, the volumetric linepack increased from 310.0 $Mm^3$ to 339.8 Mm3, a 29.8 Mm3 increase. In the NG 2018 case, the linepack rose from 346.9 to 366.3 $Mm^3$ during the same period, a 19.4 $Mm^3$ increase. Also, between the hours 14 to 23, the volumetric linepack in 100 % $H_2$ case drop from 332.9 to 309.9 $Mm^3$, a 23 $Mm^3$ drop. In the same period, the NG 2018 case linepack dropped from 352.9 to 344.1 $Mm^3$, a 8.8 $Mm^3$ drop.

#### 4.1.3. Compressor operation

Fig. 8 demonstrates compressor operation by comparing three factors: the compressor stations' total energy consumption, average utilisation, and gas flow rate passing through the station. Average utilisation is the ratio between each compressor's average and maximum possible energy consumption.

In the NG 2018 case, the compressors consume 3520 MWh of energy. In the NG 2035 case, the compressors have a total energy consumption of 1593 MWh, and in the 20 % Centralised Injection, this total increases further to 1804 MWh. In the 100 % $H_2$ case, compressors have a significantly larger energy consumption of 6350 MWh.

In the NG 2035, 20 % Centralised and Distributed Injection cases, compressors in Scotland have much lower energy consumption than the NG 2018 case. Moreover, Aberdeen and St Fergus compressors have a combined energy consumption of a third that of in the NG 2018 case. Lower energy consumption is directly linked to a lower regional gas flow rate. The assumptions regarding the supply of gas were different in NG 2018 case compared to the rest of the cases. As seen in Fig. 8 (b) and (c), gas flow through St Fergus and Aberdeen was assumed to be reduced substantially in both the 20 % Centralised and 20 % Distributed Injection cases compared to the NG 2018 case. This is because, in 20 % of Centralised and Distributed Injection cases, the gas supply from the St Fergus terminal is only 40 % that of the supply in the NG 2018 case.

In the 100 % $H_2$ case, it is assumed that compressor energy consumption is not limited by existing installed capacity, and therefore, as shown in Fig. 8 (d), the compressor utilisation can go above 100 %. Despite this relaxation, most compressor stations handled large flow rates in the 100 % $H_2$ case without exceeding the maximum possible energy consumption levels. Fig. 8(d) shows that King's Lynn and St Fergus have an energy consumption larger than the existing installed capacity, caused by the exceptionally high volumetric flowrates from St Fergus and Bacton supply points.

### 4.2. $H_2$ content at different nodes of the gas network

#### 4.2.1. $H_2$ gas content at the national level

Fig. 9 is a population diagram demonstrating the $H_2$ gas content of all the demand nodes in the 20 % Centralised and the 20 % Distributed

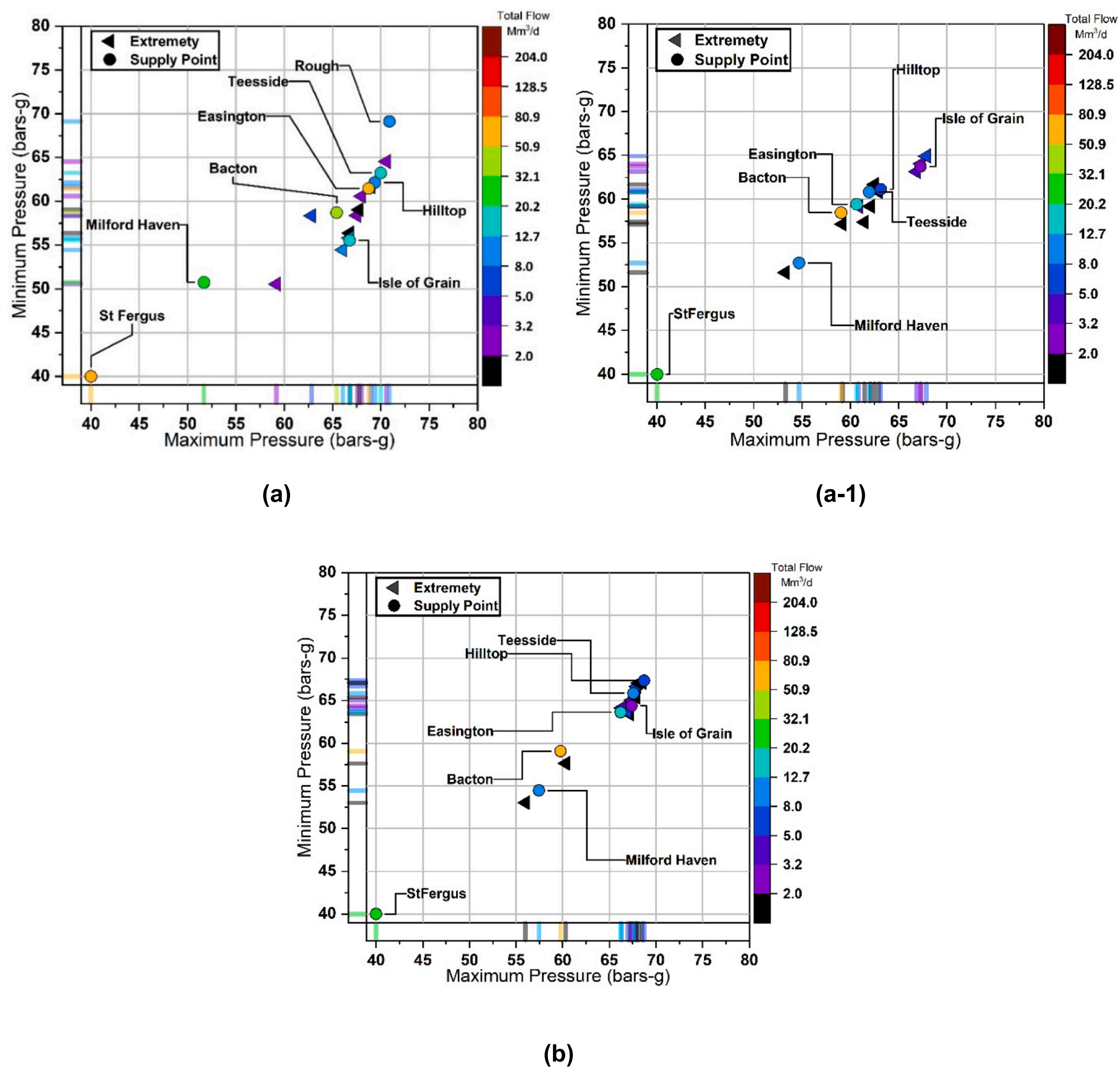


**Fig. 6.** Comparison of maximum and minimum pressures of the extremities and supply points (a) in NG 2018 case, (b) in 20% Centralised Injection case, (c) in 20% Distributed Injection case and (d) in 100% $H_2$ case.

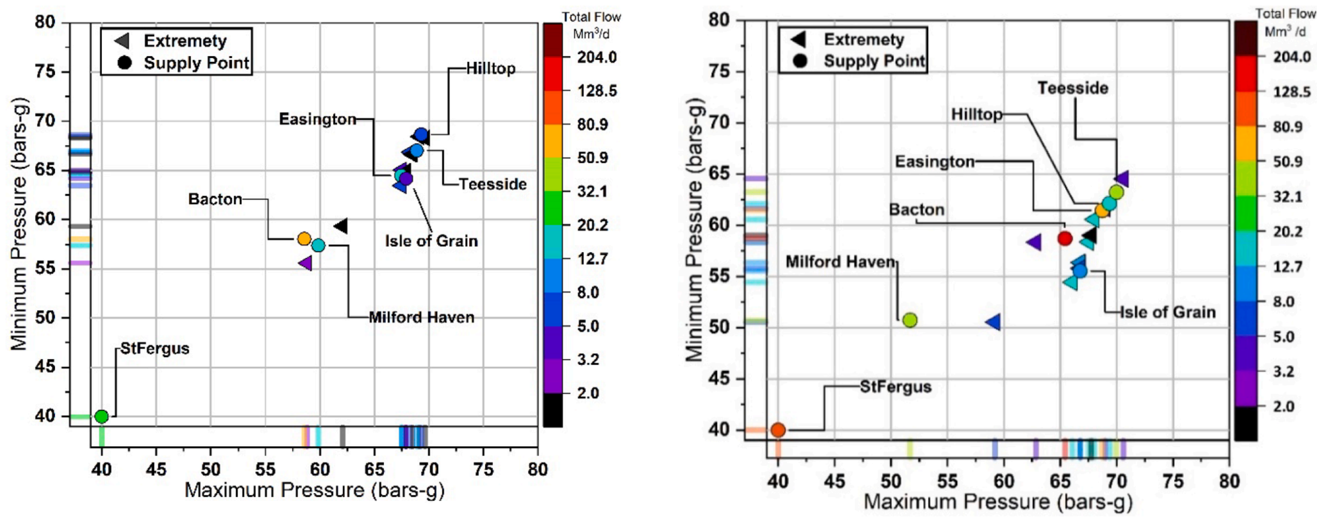


(c) (d)

**Fig. 6.** (*continued*).

Injection cases at the hour 8; the horizontal axis shows the percentage of the nodes with the same range of volumetric percentage of $H_2$ gas. Time-step t = 8 was chosen since the peak demand of the network occurs at this time step. The figure demonstrates that the 20 % Centralised Injection case is more successful in keeping $H_2$ gas in the network below 25 % volumetric compared to 20 % Distributed Injection case. Moreover, in 20 % Centralised Injection, 85 % of nodes have an $H_2$ gas content of 20–25 %. In the 20 % Distributed injection case, the $H_2$ gas content varies from 0 to 60 % by volumetric range. The largest group of nodes has a $H_2$ gas content between 10–15 % volumetric; however, this group only comprises 22 % of all nodes.

#### 4.2.2. $H_2$ gas content of every region of GB

Figs. 10 and 11 are boxplot diagrams, with each boxplot demonstrating the $H_2$ content of each demand node during the 24-hour simulation. Additionally, a horizontal line appearing inside the boxplot represent the median of $H_2$ content in each demand node. The Y-axis on the right-hand side of Figs. 9 and 10 measures the standard deviation of $H_2$ gas content in every region during the 24-hour simulation. Fig. 10 demonstrates the results of Centralised Injection case. Fig. 11 demonstrates the $H_2$ gas content under the 20 % Distributed Injection case.

According to Fig. 10, most nodes in the 20 % Centralised Injection case have a consistent $H_2$ content during the 24-hour simulation, remaining at 20 % volumetric during the day. Therefore, the median line and the narrow boxplot for most nodes are superimposed on each other. The largest standard deviation of $H_2$ content belongs to the Scotland region and the Northeast region, with a value of 0.8 each, and the smallest is 0.04, which belongs to the Midlands & East region.

The $H_2$ variations in the 20 % Distributed Injection cases are more complex and need further analysis. To better understand Fig. 11, three characteristics need to be discussed for every region: 1) the largest variation of $H_2$ gas content over time; 2) the technical $H_2$ gas limit violation, which is the ratio of nodes in each region with an $H_2$ content above the technical, operational limit (20 % volumetric); 3) the homogeneity of gas composition; which is analysed using standard deviation of $H_2$ content in every region.

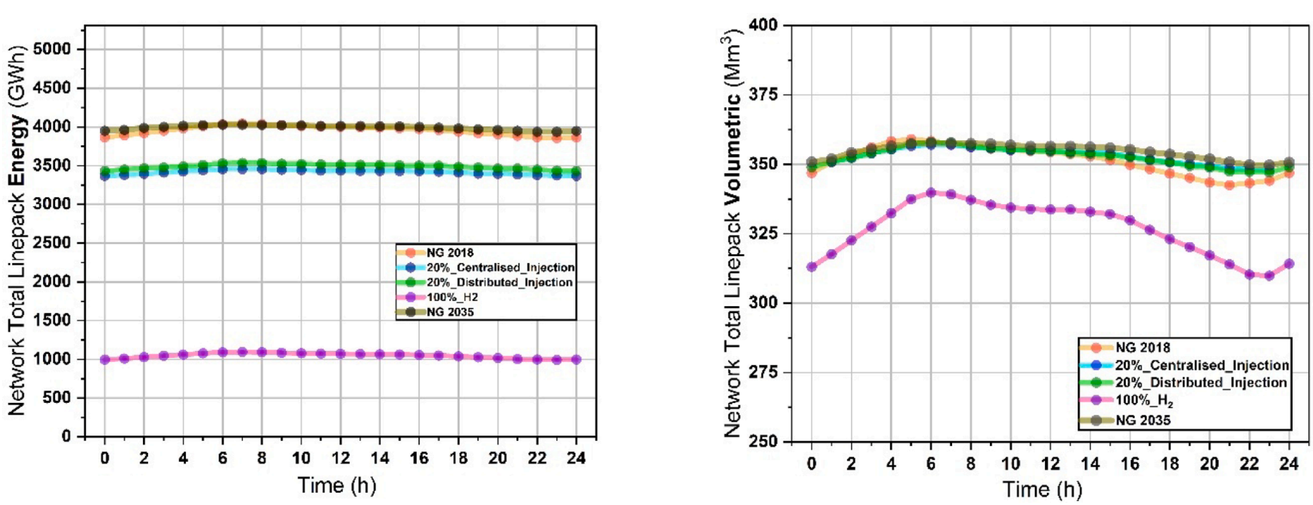


(a) (b)

**Fig. 7.** Linepack levels (a) in energy terms and (b) in volumetric terms.

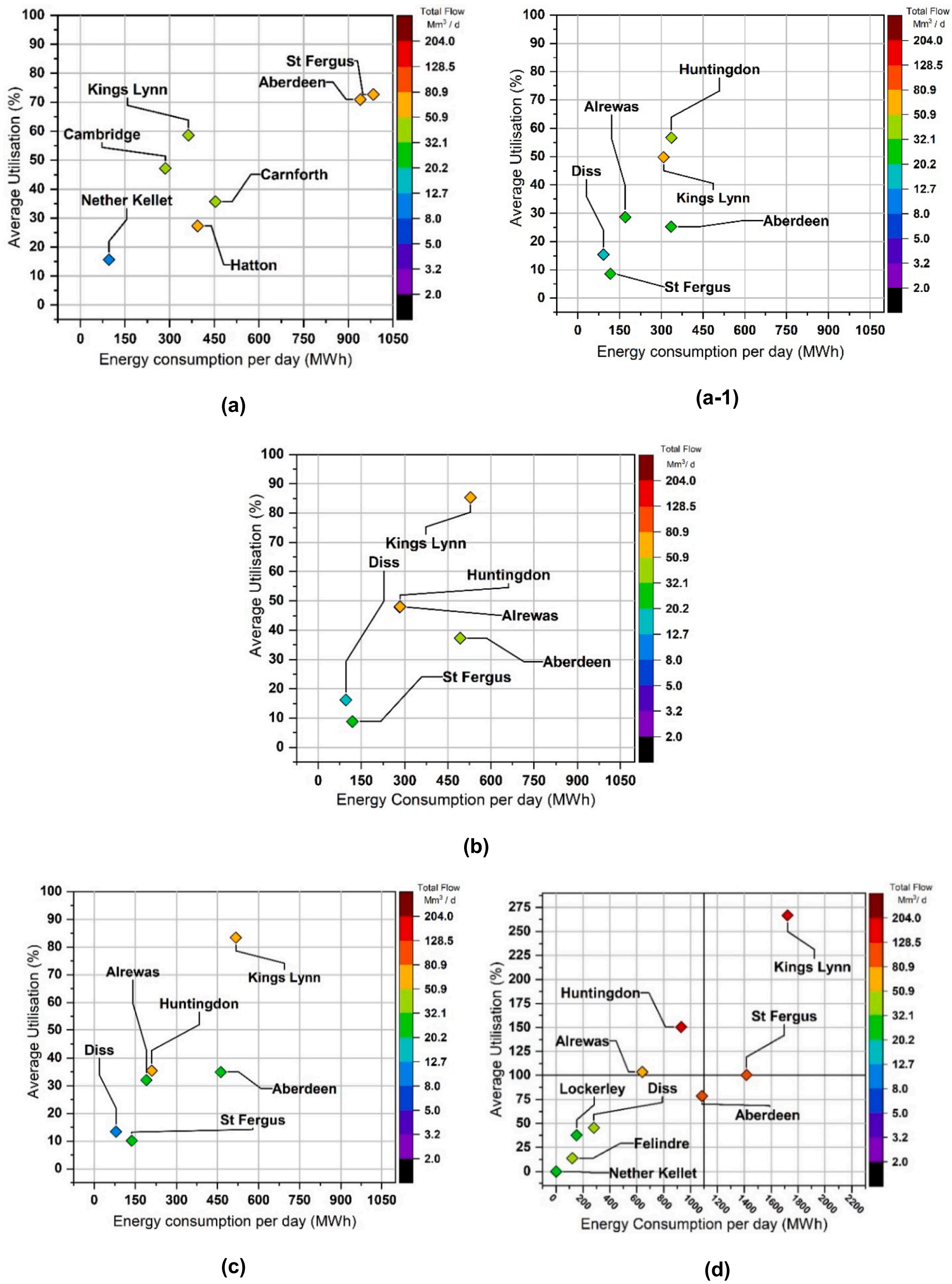


**Fig. 8.** Compressor energy consumption for 24 h, (a) in NG 2018 case, (b) in 20% Centralised Injection case, (c) in 100% $H_2$ case and (d) in 20% Distributed Injection case.

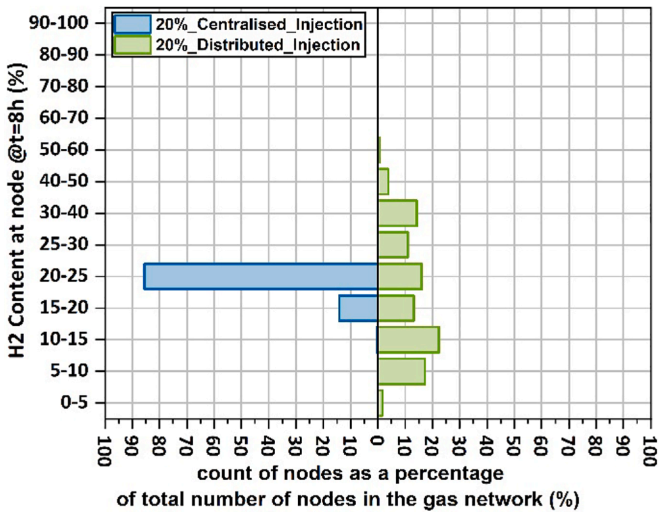


**Fig. 9.** Population diagram of volumetric percentage (%) of $H_2$ at nodes of the gas network.

*4.2.3. Largest variation of $H_2$ gas content over time*

In the 20 % Distributed Injection case, all regions host nodes with varying $H_2$ gas content over time. Also, most nodes in these regions have different $H_2$ gas content compared to each other, as evident in Fig. 11. The largest variation occurs in a node located in South Wales. Over the 24 h of simulation, the H2 content in this node varies by 38 % by volume.

The variations in four other regions are also high. The Scotland region hosts nodes with up to 24 % volumetric variations in $H_2$ gas content, followed by the South East region with 18 % and the North West region with 13 % variations in a single node. In these regions, the large variations are caused by the geographical location of $H_2$ injection points. Furthermore, as $H_2$ injection points are distant from the natural gas supply points, the flow rate of the natural gas supply and $H_2$ gas injection do not match at every time step, causing variations.

Two regions, however, have small variations; the largest $H_2$ gas content variation in nodes located Midlands & East region is only 5 % volumetric. Also, the largest $H_2$ gas content variation in nodes located in the North East region is only 4.9 % volumetric. In the Midlands & East region, variations are small because injection points are geographically located close to supply points in the region. In the North East region however, variations are even smaller, because there is no functioning compressor during the simulation, and most of the injection points are also geographically close to natural gas supply points.

*4.2.4. Technical $H_2$ gas limit violation*

The technical $H_2$ limit of 20 % volumetric should not be violated in any instance in the network. The $H_2$ gas limit violation characteristic in each region is defined as the percentage of nodes of the region with a maximum $H_2$ content above the 20 % volumetric limit.

Most of the regions violate this limit, In the South West and the North East regions, over 70 % of the nodes have an $H_2$ content above 20 % volumetric. The figures are also high in the Scotland, the South West and the South East regions, where all have above 50 % of the nodes with $H_2$ content above the limit. Two regions have small violations; only 17.5 % of nodes in the North West region are above 20 % volumetric, and in the Midlands & East region only 4 % of the nodes violate the limit.

The regions with large violations have $H_2$ gas injection points in pipelines far away from supply terminals. This resulted in a high concentration of H2 gas in some branches while also causing a low concentration of $H_2$ gas in others. Also, the regions in the second category have a total over-supply of $H_2$ gas due to the many $H_2$ gas injection points in these regions. On the other hand, there is a total under-supply of $H_2$ gas in the North West and Midlands & East regions due to the lack of $H_2$ gas injection points in these regions.

*4.2.5. Homogeneity of gas composition*

The other important characteristic is the homogeneity of $H_2$ content in each region. This is different from the previous characteristics, as it measures the level of similarity of the $H_2$ content across nodes of each region, disregarding how high or low the overall $H_2$ content is. Furthermore, regional homogeneity is measured by each region's standard deviation of $H_2$ gas content.

South Wales has the highest standard deviation of 16.4 %. This standard deviation is caused by both high node variations and many nodes with zero $H_2$ content.

North East, North West, Scotland, South East, and South West regions have standard deviations between 6.2–11.2 %. Like South Wales, these regions do not have homogeneous gas content; however, since they have no nodes with absolute zero $H_2$ content, their standard deviation decreases substantially.

The Midlands & East region has the lowest standard deviation of 3.1 %. Therefore, it can be argued that only the Midlands & East region has a gas composition that can be described as homogeneous. This is because the Midlands & East region hosts the Bacton supply terminal, which has the largest natural gas supply flow. This abundance of natural gas supply and presence of $H_2$ gas injection points close to the Bacton supply point resulted in a low standard deviation of $H_2$ content.

The homogeneity of $H_2$ gas in a region is only related to the proximity of an $H_2$ gas injection point to a supply terminal or the primary location of the gas supply to the region. Regions with low standard deviation, like Midlands & East region, have $H_2$-injection points close to the Bacton supply point, while in the rest of the regions, some of the $H_2$ injection points are located on pipelines away from the main supply point.

## 5. Conclusions

The conclusions drawn from the case studies are listed as below:

- The case studies demonstrated that the high-pressure gas network at its existing stage could host 20 % volumetric $H_2$ without compromising operating pressure levels and compressor energy consumption, regardless of the mode of $H_2$ gas injection. Linepack levels are also not significantly affected by the presence of 20 % volumetric $H_2$ gas; this was the same for both injection case studies.
- The mode of $H_2$ gas injection into the grid significantly affects the levels of $H_2$ gas at each node of the network. In the 20 % Centralised Injection case, the daily rate of $H_2$ gas injection at each node was volumetrically proportional to the natural gas entering the network from the related supply node, and the daily rate was set at 20 % volumetric. This centralised injection of $H_2$, led to a homogenous mix of $H_2$ and natural gas across the network. This was not the case in the 20 % Distributed Injection case, and $H_2$ gas injection was proportional to the generation capacity of windfarms corresponding to the location of $H_2$ gas injection. This distributed injection of $H_2$ gas led to a non-homogenous mix of $H_2$ and natural gas across the network.
- For 100 % $H_2$ transmission, pressure levels can be kept as the same as the existing levels. However, to transport 100 % $H_2$ gas, a significantly large compressor energy consumption will be required, up to 3.9 times that of typical levels in the existing network. By keeping the pressure levels the same as existing levels, linepack levels will drop to a quarter of the existing linepack levels. This means the network will have much lower within-day flexibility than today.

This research can be further developed by finding accurate means of simulating $H_2$ gas injection into the high-pressure grid, especially for the $H_2$ gas generated from intermittent and variable sources like wind and solar. Furthermore, by developing a real-time simulation method that

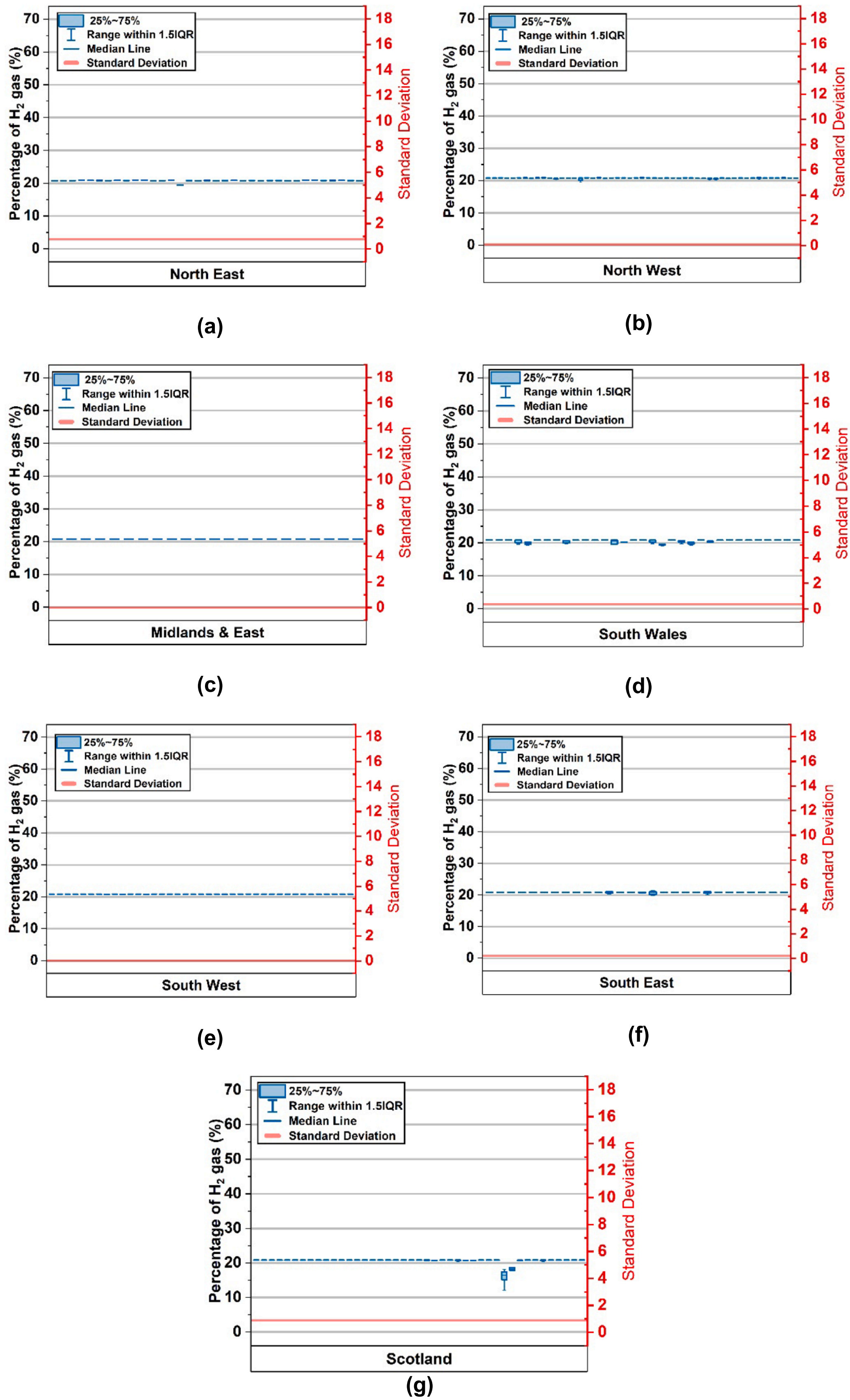


**Fig. 10.** $H_2$ gas content at each node at each time-step of the simulation in the 20% Centralised Injection case.

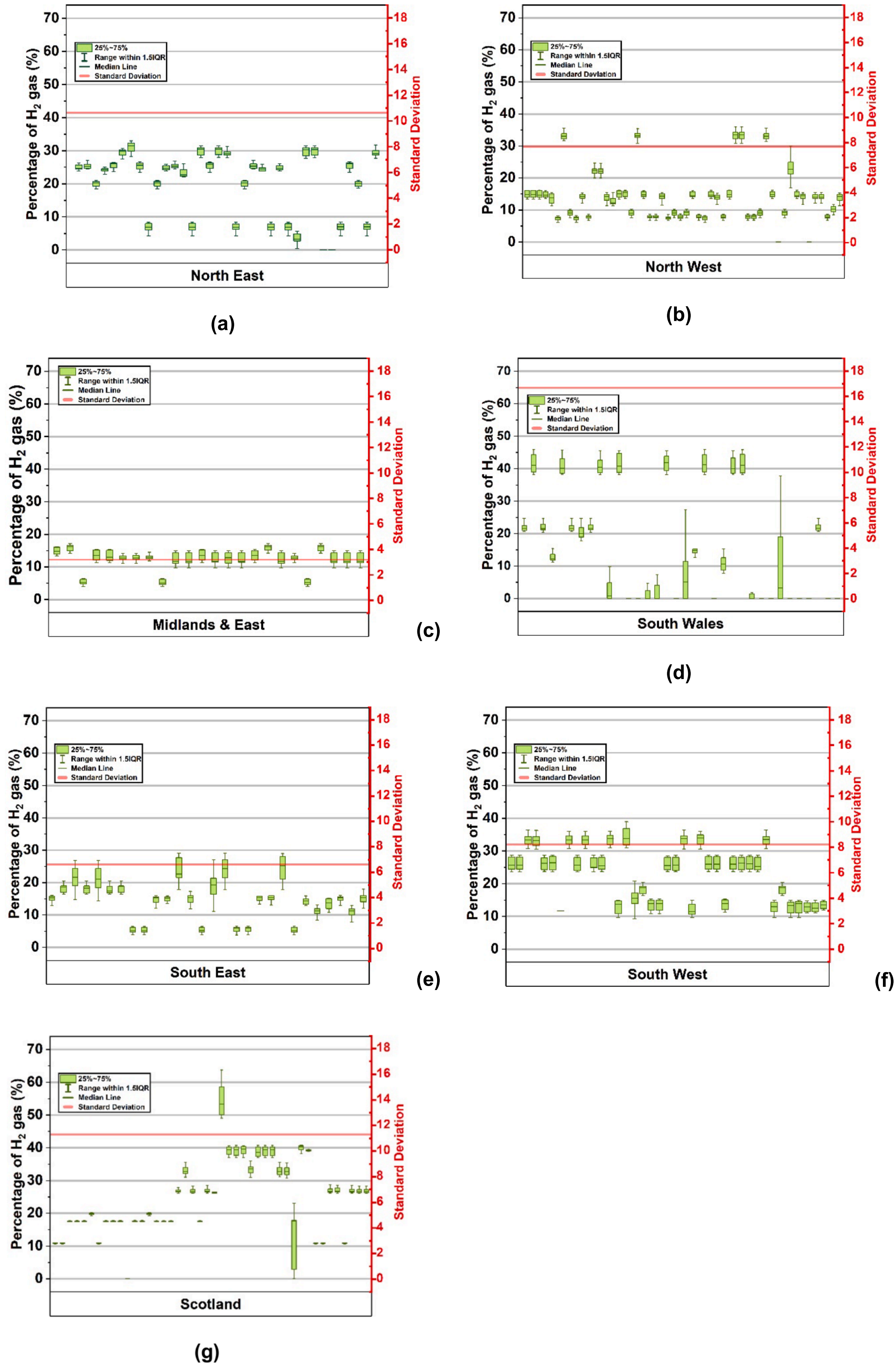


**Fig. 11.** $H_2$ gas content at each node at each simulation time-step under 20% Distributed Injection case.

monitors gas flow in every time-step, the $H_2$ gas content in the network can be actively measured, and $H_2$ gas can be injected according to these two parameters. Also, there needs to be more focus on optimising the location of $H_2$ gas injection so that $H_2$ gas reach-out and homogeneity improve in various regions of the high-pressure gas network.

Additionally, as linepack levels in the 100 % $H_2$ case are significantly lower than existing levels, the within-day flexibility of the gas network will be compromised. It is, therefore, crucial to know how the gas network's resilience to external events will be compromised when transporting 100 % $H_2$ gas. Also, it is crucial to understand how the network's reliability will be compromised when facing system difficult operational situations.

## CRediT authorship contribution statement

**Amirreza Azimipoor:** Writing – original draft, Visualization, Validation, Methodology, Formal analysis, Conceptualization. **Tong Zhang:** Writing – review & editing, Methodology, Conceptualization. **Meysam Qadrdan:** Writing – review & editing, Supervision, Resources, Project administration, Funding acquisition, Conceptualization. **Nick Jenkins:** Writing – review & editing, Supervision, Project administration, Funding acquisition.

## Declaration of competing interest

The authors declare the following financial interests/personal relationships which may be considered as potential competing interests: Meysam Qadrdan reports financial support was provided by Engineering and Physical Sciences Research Council. Amirreza Azimipoor reports financial support was provided by Engineering and Physical Sciences Research Council. Tong Zhang reports was provided by Engineering and Physical Sciences Research Council. Nick Jenkins reports financial support was provided by Engineering and Physical Sciences Research Council.

## Acknowledgements

This work was supported by the Engineering and Physical Sciences Research Council (EPSRC), United Kingdom through grants EP/X038823/1 (HI-ACT) and EP/S001492/1 (MISSION).

## Appendix I. Validation of the modelling results

The appendix validates the model outcomes by initially outlining the selection of input data for the model and subsequently comparing the results with real data.

Data of nodal pressure levels of the GB high-pressure gas network is not available. Therefore, the initial nodal pressure levels used in the simulation are approximations, guessed based on the pressure operational range of pipelines of the network.

However, the hourly linepack levels of the network are publicly available at National Gas database [52]. The hourly linepack levels are reported both as aggregated network linepack and broken down for twelve geographical zones of network.

As linepack is a parameter representing pressure levels in pipelines. Also, the change in the hourly linepack level of the network is a function of changes in supply and demand of the network. Therefore, linepack is a parameter that can represent all the model outputs.

By comparing the result linepack with real linepack, it is demonstrated that all the model attributes represent reality, demonstrating the validity of the model results.

### *A. Choosing the input data*

The winter season used for developing the gas network model starts from October 2018 to the end of March 2019. This is the last winter season before the COVID-19 pandemic, marked by moderate gas consumption for heating and electricity generation. The winter seasons after the COVID-19 pandemic were not chosen because the Russia-Ukraine war caused significant changes to supply and demand patterns. In the chosen winter season, like all winters before it, the UK continental shelf is the primary source of natural gas supply, and a significant portion of GB gas comes through the St Fergus supply point in Scotland.

Fig. 12 (a) demonstrates the gas supply in the winter season using box and whisker diagrams. In winter, natural gas is supplied mainly from the UK continental shelf. The mean supply from the continental shelf is 198 Mm3/d. LNG is the second primary source of natural gas; however, the season's mean LNG supply is less than 1/10 that of the season's mean gas supply from the shelf.

Fig. 12 (b) demonstrates the winter season gas consumption by type of offtakes using box and whisker diagrams. As seen in Fig. 2, gas is mainly sent to LDZ networks, eventually used for heating. The mean gas used by LDZs is 122 Mm3/d. However, the gas use by power generation using CCGTs is also significant, with a mean gas consumption of 114 Mm3/d. Industrial sites use a small portion of gas, and almost no gas is injected into storage sites or exported.

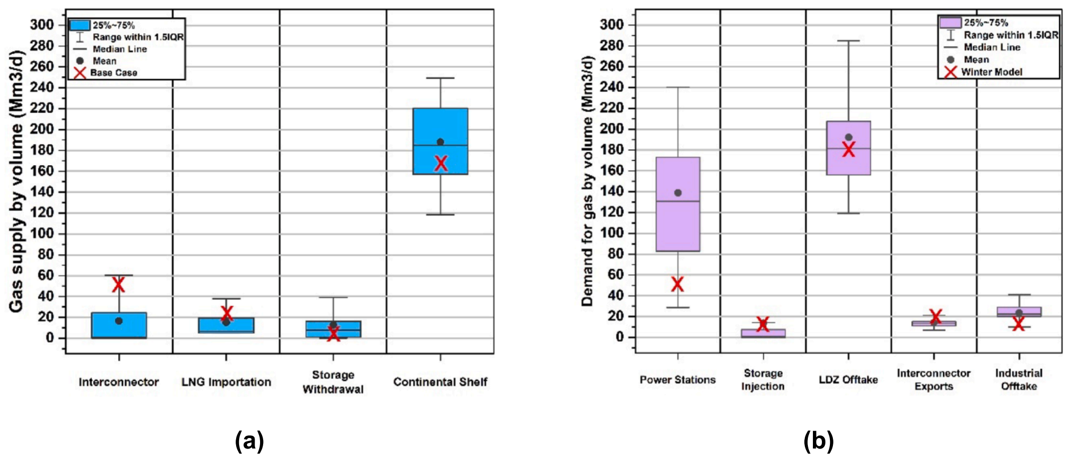


**Fig. 12.** Supply and Demand in Winter Season 20182019

The winter day of 25th November 2018 was chosen for modelling since the supply and demand of gas on this day follows the same trend as the winter season of 2018–2019. In Fig. 12 (a) and (b), the X mark on each boxplot marks the level on 25th November 2018. On this day, St Fergus in Scotland is the leading gas supplier to the network, followed by Easington in the Northeast. Because of this, the gas flows from the network's North towards the South and from the East side to the West.

*B. Comparing results to real data*

Fig. 13 depicts the entire model's hourly linepack against the seasonal linepack range. Furthermore, the figure shows that the start-of-the-day and end-of-the-day linepack in the NG 2018 case is 346.9 $Mm^3$. The linepack swing is the difference between the maximum and minimum linepack in the day, which is 16.6 $Mm^3$.

Three values were measured to quantify the model's calibration state. The first value is the population of the result hourly linepack that falls within the season's range. The second value is the maximum deviation of the result hourly linepack from the season's range's median. The final value is the minimum deviation of the result hourly linepack from the season'thes range's median. In both models, 100 % of the population of result hourly linepack falls within the season's range. In the NG 2018 case, the largest deviation from the season's median is 2.1 %, while the smallest deviation from the season's median is 0 %.

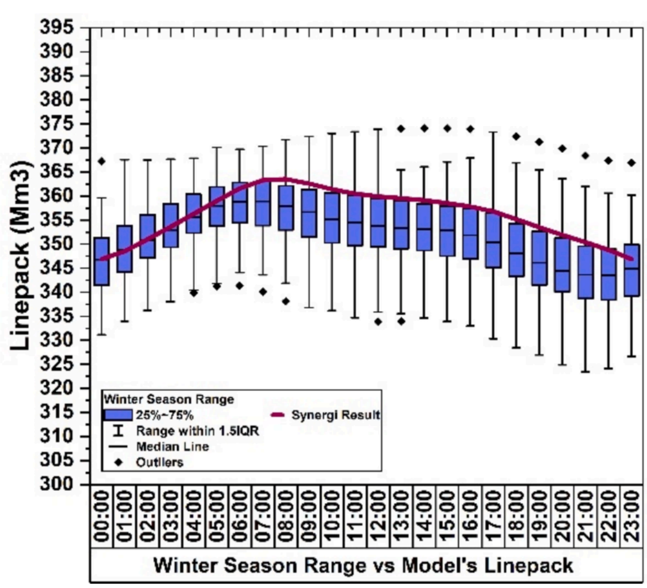


**Fig. 13.** Model's total Linepack vs Season's Range

The calibration status of the model further evaluated for every linepack zone, but due to the vast number of zones, the results have been summarised in Fig. 14. Furthermore, Fig. 14 reports three attributes for each linepack zone: (1) the population of result linepack in range; (2) the largest linepack deviation from the range's median; (3) the smallest linepack deviation from the range's median. Fig. 14. indicates that out of the twelve zones in the NG 2018 case, nine have all hourly linepack within the expected range for the season. Among the zones within range, the maximum deviation from the median ranges from 8 % to 2.4 %, while the minimum deviation ranges from 0 % to 2.5 %.

Fig. 14 also shows that three zones with out-of-range results: Zone 2 in Scotland, Zone 4 in Northwest England, and Zone 11 in South Wales. In Zone 2, none of the linepack results fall within range, with a maximum deviation from the median of 10.1 % and a minimum deviation of 7.5 %. In Zone 4, only 12.5 % of results are within the seasonal range, with a maximum deviation of 21 % and a minimum deviation of 17 %. Finally, in Zone 11, none of the results fall within the range, with a maximum deviation of 27 % and a minimum deviation of 25 % from the seasonal range.

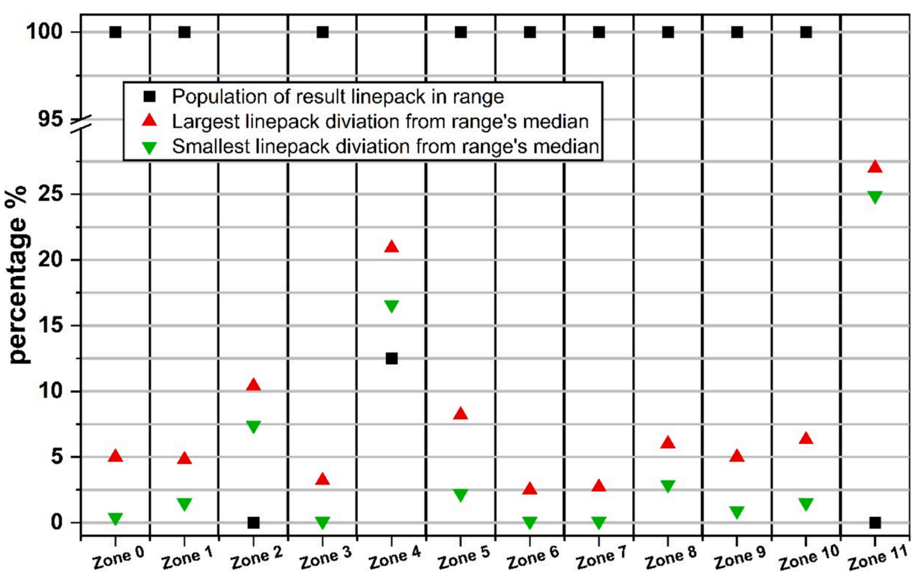

**Fig. 14.** Linepack in every Linepack Zone of the NG 2018 case.

Fig. 15 shows box plots representing the pressure levels. Each box stretches across the full range of pressures of the node it represents during the 24-hour long simulation, stretching from the minimum to the maximum pressure level of the node. Since the number of datasets is small, no whiskers or outliers were used in these graphs. The dotted lines at the two ends of the Y axes demonstrate the maximum and minimum operating pressure of the pipelines in that zone. This operating pressure range is defined by National Gas; however, it is not publicly available data.

Although the model linepack in zones 2,4, and 11 deviates from the winter season's range, according to Fig. 14, their pressure levels are all in the operating range. In addition, since the total linepack is within seasonal range (Fig. 13), the model produces results reasonably reflecting within-day changes to the operational attributes of the whole system. Therefore, the model is suitable for the study conducted in this journal paper.

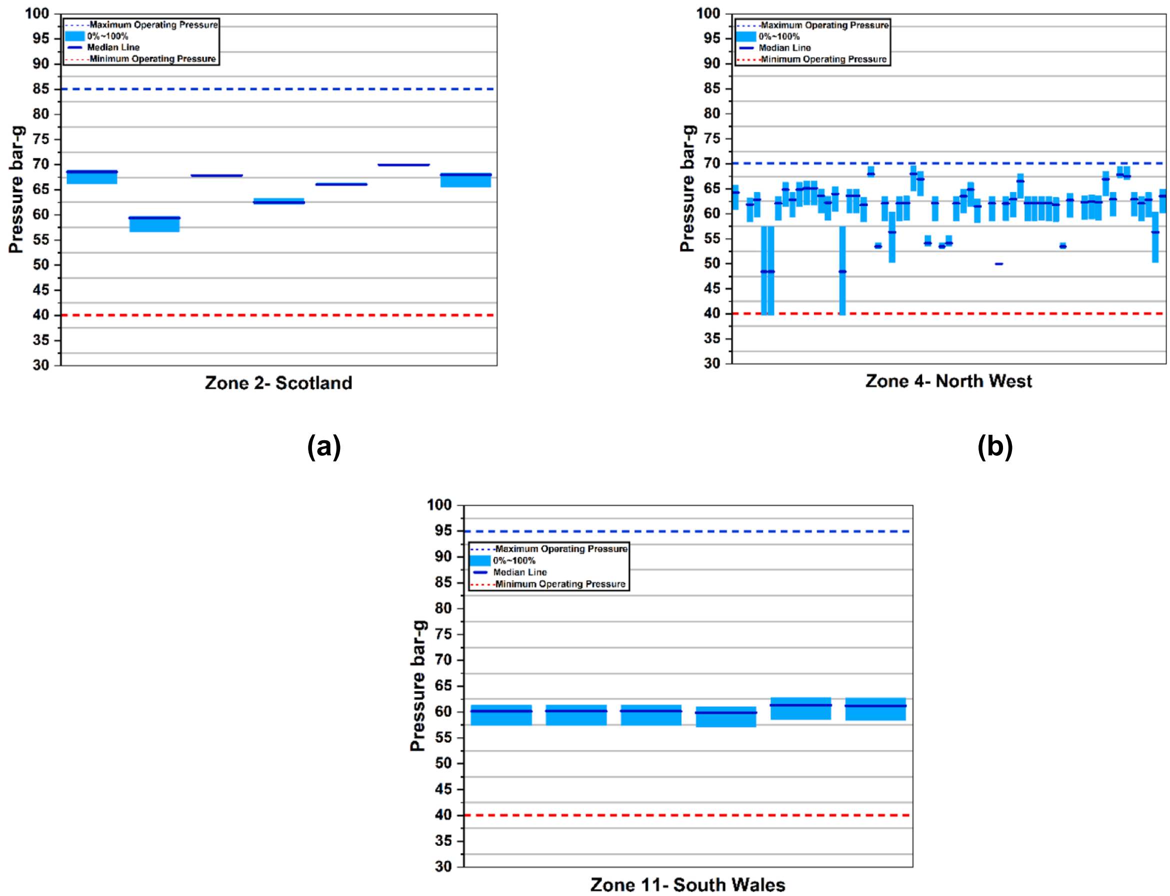


(c)

**Fig. 15.** Pressure levels of nodes in (a) Zone 2, (b) Zone 4 and (c) Zone 11.

### C. *Summary*

The aggregated linepack, as well as eight zonal linepack levels are assessed to be within-range. The three zonal linepack levels that are not in range, have pressure levels within the operational range. Therefore the modelling results are reasonably reliable.

## Appendix II. Sensitivity analysis of model parameters

A sensitivity analysis has been conducted to establish the robustness of the results obtained from the model. More specifically, the study aimed at analysing the sensitivity of pressure and linepack to variations in H2 concentration in the gas supplied.

### A. *The case study scope*

This analysis utilised parts of Scotland region of the GB high-pressure gas network model as shown in Fig. 16 (zone 0 in the map in Fig. 1.).

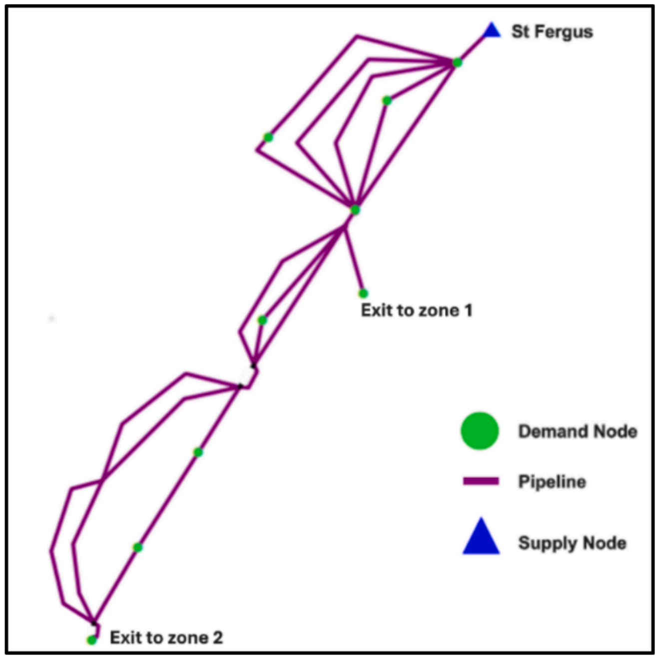


**Fig. 16.** Map of zone 0 in Scotland region of GB high-pressure gas network used for sensitivity analysis.

*B. The assumptions*

Time is assumed to be fixed at t = 6 h, at a timestep at which gas demand is equal to gas supply in the network. analysis. Another assumption made, is that all the pipelines have diameter of 900 mm. These two assumptions created a fully controlled environment for the sensitivity analysis.

The model has one supply node, St-Fergus, with a fixed pressure of 70 bar-g and nine demand nodes with a fixed energy demand. Two of these demand nodes are located at the zone exit points, simulating gas that exist zone 0 into zones 1 and 2.

No compressors were used in this analysis. The assumptions are depicted in Table 10.

**Table 10**
List of elements used.

| Type of element | Input | Output |
|---|---|---|
| Supply Node | Fixed pressure @70 bar-g | Volumetric flow |
| Demand Nodes | Fixed demand in energy terms | Volumetric flow<br>Pressure level |
| Pipeline | Diameter of all pipes 900 mm<br>Length (km)<br>Roughness of all pipes 0.067 mm | Linepack |

Demand and Supply of gas at t = 6 h in the model are equal to 18.9 GWh.

| Distance from supply point (km) | Node name | Demand GWh |
|---|---|---|
| 0.1 | St-Fergus industrial | 0.001 |
| 26.24 | Kinknockie | 0.001 |
| 77.8 | Burnhervie | 0.4 |
| 89.2 | Aberdeen | 0.2 |
| 91 | Exit to Zone 1 | 5.9 |
| 151.06 | Careston | 0 |
| 182.12 | Balgray | 0.2 |
| 255.8 | Drum | 0.3 |
| 288.16 | Exit to Zone 2 | 11.9 |

The composition of gas has been varied in six steps. $H_2$ and natural gas have been considered. Natural gas is a composition of five gases, and all of them are scaled according to the step-variation as depicted in Table 11.

**Table 11**
Step-variations in gas composition.

| Step-variation | Volumetric % of $H_2$ | Volumetric % of Natural Gas |
|---|---|---|
| 1 | 0 | 100 |
| 2 | 5 | 95 |
| 3 | 10 | 90 |
| 4 | 15 | 85 |
| 5 | 20 | 80 |
| 6 | 100 | 0 |

*C. Results and discussion*

In Fig. 17 the Y axis demonstrates the difference between the pressure of each node compared to the 0 % $H_2$ case. The X-axis shows the distance between the demand node and the St-Fergus supply point. This distance is calculated by measuring the length of pipeline that gas travels to reach the demand node.

Fig. 17 shows that as the vol % of $H_2$ increases, the pressure degradation due to distance exacerbates and pressure levels drop at a faster rate.

Fig. 17 also shows that pressure degradation in exit node to zone 1 has a sharp rise. And as $H_2$ level in the network increases, this degradation increases further.

For instance, when network has 5 % $H_2$ content, the node immediately before exit node to zone 1, has a degradation of −0.05 bar-g and at the exit node to zone 1, this increases to −0.11 bar-g. However, when the network has 100 % $H_2$, the node immediately before exit node to zone 1, has a degradation of −0.52 bar-g and at the exit node to zone 1, this increases to −1.52 bar-g.

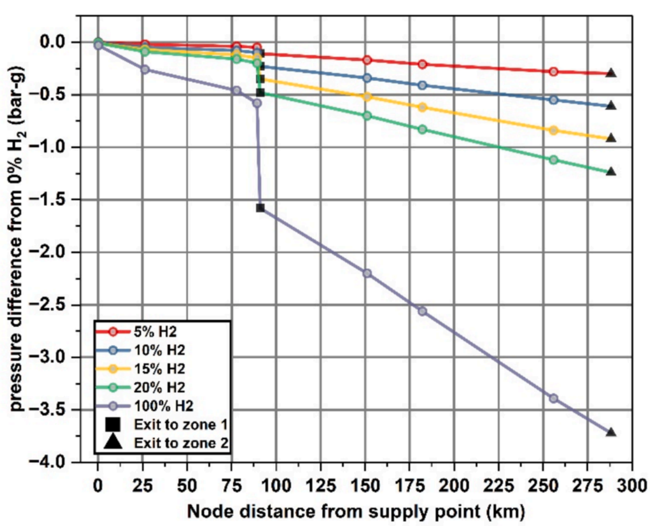


**Fig. 17.** Pressure vs. distance from supply point.

Fig. 18 depicts the difference between the linepack of each case compared to 0 % $H_2$ case; the Y-axis is the difference in energy terms and the X-axis is the difference in volumetric terms.

Fig. 18 demonstrates that as vol% of $H_2$ gas increases, both linepack levels drop. This outcome arises from the greater pressure degradation experienced in networks with elevated $H_2$ content, which reduces volumetric linepack.

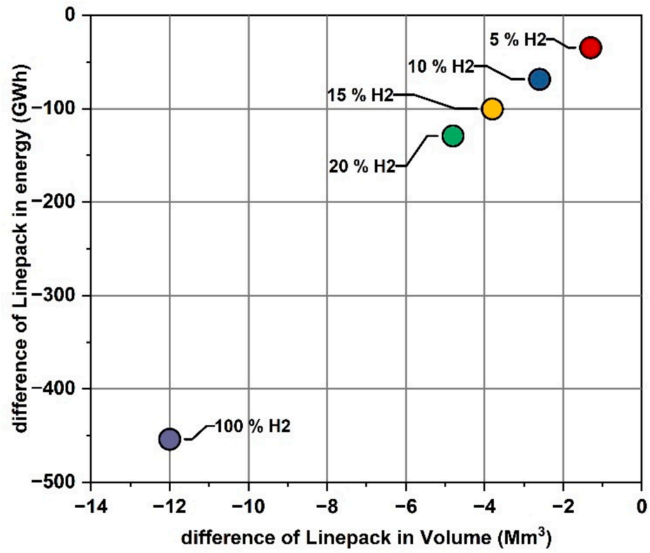


**Fig. 18.** Linepack in the model.

*D. Summary*

The sensitivity analysis shows: (1) As the vol % of $H_2$ increases, the pressure degradation due to distance exacerbates and pressures drop at a faster rate. (2) As the pressure degradation is larger with H2 gas compared to natural gas, the volumetric linepack is expected to be lower.

## Data availability

Data related to structure and physical aspects of the GB gas network, pipelines and compressor stations are confidential. Data of gas consumption, supply and linepack are public provided in reference.

## References

[1] UNFCCC. The Paris Agreement 2018. https://unfccc.int/process-and-meetings/the-paris-agreement (accessed July 12, 2024).
[2] UK Government. The Climate Change Act 2008 (2050 Target Amendment) Order 2019 2019.
[3] European Commission. European Climate Law 2021. https://climate.ec.europa.eu/eu-action/european-climate-law_en#:~:text=The%20European%20Climate%20Law%20sets,greenhouse%20gas%20emissions%20by%202050. (accessed July 12, 2024).
[4] Hydrogen UK. International Hydrogen Progress Index. 2023.
[5] European Commission. Supporting Clean Hydrogen n.d. https://single-market-economy.ec.europa.eu/industry/strategy/hydrogen_en (accessed July 12, 2024).
[6] National Grid. Future Energy Scenarios 2022. http://fes.nationalgrid.com.
[7] Reyes-Bozo L, Fúnez-Guerra C, Luis Salazar J, Vyhmeister E, Valdés-González H, Jaén Caparrós M, et al. Green hydrogen integration in aluminum recycling: techno-economic analysis towards sustainability transition in the expanding aluminum market. Energy Convers Manage: X 2024;22:100548. https://doi.org/10.1016/j.ecmx.2024.100548.
[8] BEIS. UK hydrogen strategy. vol. 85. 2021. https://doi.org/10.1002/cind.859_6.x.
[9] Menon NV, Nguyen VB, Quek R, Kang CW, Zhang B, Chan SH. Modelling guided energy management system for a hydrogen–fuelled harbour tug. Energy Convers Manage: X 2024;23:100642. https://doi.org/10.1016/j.ecmx.2024.100642.
[10] Julian Wettengel. EU sets state support conditions for German gas and hydrogen power plants 2023. https://www.cleanenergywire.org/news/eu-sets-state-support-conditions-german-gas-and-hydrogen-power-plants-econ-min (accessed July 12, 2024).
[11] Hydrogen Europe. Use of Hydrogen in Buildings. 2022.
[12] Hydrogen UK. Hydrogen Storage: Delivering on the UK's Energy Needs. 2022.
[13] EU Science Hub. Blending hydrogen into the EU gas system 2022. https://joint-research-centre.ec.europa.eu/jrc-news-and-updates/blending-hydrogen-eu-gas-system-2022-01-19_en (accessed July 12, 2024).
[14] ACER. Repurposing existing gas infrastructure to pure hydrogen: ACER finds divergent visions of the future | www.acer.europa.eu 2021. https://www.acer.europa.eu/news-and-events/news/repurposing-existing-gas-infrastructure-pure-hydrogen-acer-finds-divergent-visions-future (accessed April 22, 2023).
[15] Wolf N, Kühn L, Höck M. International supply chains for a hydrogen ramp-up: techno-economic assessment of hydrogen transport routes to Germany. Energy Convers Manage: X 2024;23:100682. https://doi.org/10.1016/j.ecmx.2024.100682.
[16] Van Rossam R, Jens J, La Guardia G, Wang A, Kühnen L, Overgaag M. European Hydrogen Backbone. 2022.
[17] Leigh Collins. German hydrogen pipeline network will begin transporting H2 in 2025, with 9,700km in place by 2032, says government 2023. https://www.hydrogeninsight.com/policy/german-hydrogen-pipeline-network-will-begin-transporting-h2-in-2025-with-9-700km-in-place-by-2032-says-government/2-1-1554455 (accessed July 12, 2024).
[18] Gasunie. Hydrogen pipeline in Zeeland has been proving added value for three years 2021. https://www.gasunie.nl/en/projects/hydrogen-network-netherlands#:~:text=The%20vast%20majority%20of%20the,use%20for%20three%20years%20now. (accessed July 12, 2024).
[19] National Gas. National Gas deal paves the way towards no-regrets hydrogen network 2023. https://www.nationalgas.com/news/national-gas-deal-paves-way-towards-no-regrets-hydrogen-network (accessed July 12, 2024).
[20] National Grid Gas Transmission. Gas Ten Year Statement. 2022.
[21] BEIS. Digest of the UK Energy Statistics, Chapter 4: Natural Gas. 2021.
[22] National Grid Gas Transmission. FutureGrid Progress Report 2021.
[23] National Grid Gas Transmission. Project Union: Launch Report 2022 2022.
[24] Adam P, Bode R, Groissboeck M. HYDROGEN TURBOMACHINERY Readying Pipeline Compressor Stations For 100% Hydrogen. 2020.
[25] National Gas. Closure Report Phase 1 Facility. 2024.
[26] Zabrzeski Ł, Janusz P, Liszka K, Łaciak M, Szurlej A. The effect of hydrogen transported through a gas pipeline on the functioning of gas compression station work. AGH Drilling, Oil, Gas 2017;34:959–68.
[27] Bainier F, Kurz R. Impacts of H2 blending on capacity and efficiency on a gas transport network. volume 9: oil and gas applications; supercritical CO2 power cycles; wind energy. Am Soc Mech Eng 2019. https://doi.org/10.1115/GT2019-90348.
[28] Witek M, Uilihoorn F. Impact of hydrogen blended natural gas on linepack energy for existing high pressure pipelines. Arch Thermodyn 2023. https://doi.org/10.24425/ather.2022.143174.
[29] Rowley P, Wilson G. Flexibility in Great Britain's gas networks: analysis of linepack 2019. https://ukerc.ac.uk/publications/linepack/ (accessed April 22, 2023).
[30] Wang C, Zhou D, Xiao W, Shui C, Ma T, Chen P, et al. Research on the dynamic characteristics of natural gas pipeline network with hydrogen injection considering line-pack influence. Int J Hydrogen Energy 2023;48:25469–86.
[31] Wesselink O, Krom A, van Agteren M. Balancing Hydrogen Networks Safely: A Method for Calculating Linepack Potential Without Causing Integrity Risk Due to Hydrogen-Enhanced Fatigue. International Pipeline Conference, vol. 86564, American Society of Mechanical Engineers; 2022, p. V001T08A003.
[32] Wu C, Li W, Qian T, Xie X, Wang J, Tang W, et al. Optimal scheduling of hydrogen blended integrated electricity–gas system considering gas linepack via a sequential second-order cone programming methodology. J Energy Storage 2024;76:109718.

[33] Jiang Y, Ren Z, Dong ZY, Sun Z, Terzija V. An optimal dispatch method of integrated electricity and gas systems incorporating hydrogen injection flexibility. Int J Electr Power Energy Syst 2024;155:109662.
[34] Fernandes LA, Marcon LRC, Rouboa A. Simulation of flow conditions for natural gas and hydrogen blends in the distribution natural gas network. Int J Hydrogen Energy 2024;59:199–213. https://doi.org/10.1016/j.ijhydene.2024.01.014.
[35] Khabbazi AJ, Zabihi M, Li R, Hill M, Chou V, Quinn J. Mixing hydrogen into natural gas distribution pipeline system through Tee junctions. Int J Hydrogen Energy 2024;49:1332–44. https://doi.org/10.1016/j.ijhydene.2023.11.038.
[36] Guandalini G, Colbertaldo P, Campanari S. Dynamic quality tracking of natural gas and hydrogen mixture in a portion of natural gas grid. Energy Procedia 2015;75: 1037–43. https://doi.org/10.1016/j.egypro.2015.07.376.
[37] Zhou D, Yan S, Huang D, Shao T, Xiao W, Hao J, et al. Modeling and simulation of the hydrogen blended gas-electricity integrated energy system and influence analysis of hydrogen blending modes. Energy 2022;239:121629. https://doi.org/10.1016/j.energy.2021.121629.
[38] Zhang Z, Saedi I, Mhanna S, Wu K, Mancarella P. Modelling of gas network transient flows with multiple hydrogen injections and gas composition tracking. Int J Hydrogen Energy 2022;47:2220–33. https://doi.org/10.1016/J.IJHYDENE.2021.10.165.
[39] Ekhtiari A, Flynn D, Syron E. Investigation of the Multi-Point Injection of Green Hydrogen from Curtailed Renewable Power into a Gas Network. Energies 2020, Vol 13, Page 6047 2020;13:6047. https://doi.org/10.3390/EN13226047.
[40] Saedi I, Mhanna S, Mancarella P. Integrated electricity and gas system modelling with hydrogen injections and gas composition tracking. Appl Energy 2021;303: 117598. https://doi.org/10.1016/j.apenergy.2021.117598.
[41] Adam P, Heunemann F, Von dem Bussche C, Engalshove S, Thiemann T. Hydrogen infrastructure-the pillar of energy transition. 2021.
[42] National Grid Gas Transmission. GFOP study: Delivering within-day customer needs now and into the future 2021. https://www.nationalgas.com/insight-and-innovation/gas-future-operability-planning-gfop/understanding-within-day-behaviour (accessed April 22, 2023).
[43] DNV. Hydraulic modelling software | hydraulic simulation software | Synergi Gas 2023. https://www.dnv.com/services/hydraulic-modelling-and-simulation-software-synergi-gas-3894 (accessed April 22, 2023).
[44] NAN Steel. Pipe Roughness n.d. https://www.nan-steel.com/news/pipe-roughness.html (accessed January 28, 2025).
[45] Lielmezs J. Comparison of benedict-webb-rubin and starling equations of state for use in p-v-t calculations of binary mixtures. Thermochim Acta 1989;152:341–58. https://doi.org/10.1016/0040-6031(89)85403-6.
[46] National Gas. Future Grid Phase 1 Closure Report 2024. https://www.nationalgas.com/sites/default/files/documents/FutureGrid%20Phase%201%20Closure%20Report%20July%202024.pdf (accessed January 28, 2025).
[47] National Grid Gas Transmission. Transmission Planning Code. 2015.
[48] National Grid Gas Transmission. St Fergus Investment Programme Engineering. n. d.
[49] Business N, Submission P. Compressor Annex Supporting Information December 2019 2019.
[50] Business N, Submission P. Annex Engineering Justification Paper December 2019 2019:1–47.
[51] National Grid Gas Transmission. Data Item Explorer n.d. https://mip-prd-web.azurewebsites.net/DataItemExplorer (accessed April 22, 2023).
[52] National Grid Gas Transmission. Data Item Explorer n.d. https://mip-prd-web.azurewebsites.net/DataItemExplorer (accessed April 22, 2023).